Geophys. J. R. astr. Soc. (1986) **87**, 917–948

A comparison of analytical and numerical results for a 2-D control model in electromagnetic induction – II. E-polarization calculations

J. T. Weaver *Department of Physics, University of Victoria, PO Box 1700, Victoria, BC V8W 2Y2, Canada*

B. V. LeQuang and G. Fischer *Observatoire Cantonal, CH-2000 Neuchâtel, Switzerland*

Accepted 1986 June 2. Received 1986 June 2; in original form 1985 December 19

Summary. The 2-D model proposed in an earlier paper as a control on the accuracy of numerical modelling programs operating in the B-polarization mode, is used here to test the corresponding E-polarization calculations. The model comprises a conducting slab divided into three segments of different conductivities and overlying a perfect conductor. The control solution is obtained in the E-polarization mode by a 'quasi-analytic' method in which a 1-D integral equation satisfied by the horizontal magnetic field on the surface of the conductor is solved by the method of successive approximations. Values of all the field components for a particular set of model parameters are calculated by this method at selected points on the surface of the conductor and on a horizontal plane inside the conductor. As in the previous paper, these values are used to check the accuracy of results given by (i) the finite difference program of Brewitt–Taylor & Weaver in which improved finite difference formulae for calculating the derived magnetic field components have been incorporated and (ii) the finite element program of Kisak & Silvester. The finite difference program gives results in remarkably close agreement with the analytic solution; relative errors in all the field components are generally less than 1 per cent. The finite element program does not perform as well. In particular it gives errors of around 10 per cent in the values of the vertical magnetic field near the segment boundaries. It appears that the finite element program is not suitable for models which have different 1-D conductivity distributions at infinity on the lhs and rhs.

Key words: electromagnetic induction, E-polarization, electrical conductivity, numerical modelling

1 Introduction

In an earlier paper (Weaver, LeQuang & Fischer 1985) – hereafter referred to as paper I – a simple control model was proposed for testing the accuracy of the various numerical modelling programs that have been devised for calculating the electromagnetic response of a 2-D conductivity structure due to a locally uniform magnetic field varying harmonically in time. In paper I we considered a B-polarization field and solved the induction problem for the control model exactly by analytical methods. The analytic results were then compared with numerical values given by finite difference (Brewitt-Taylor & Weaver 1976) and finite element (Kisak & Silvester 1975) programs applied to the same control model. We believe that all numerical programs should pass an initial test such as this before they are applied to more complicated structures, or are compared with other programs for accuracy. In this regard it is worth noting that this model has now been added to the set of test models in the Comparison of Modelling Methods in Electromagnetic Induction Problems (COMMEMI), an international project established by Working Group I-3 of the International Association of Geomagnetism and Aeronomy (Zhdanov & Varentsov 1985).

This paper is a sequel to paper I; the same control model is used to make a similar comparison of results for an E-polarization field. Unfortunately it is not possible to find a strictly analytic solution of such problems, but the solution can be expressed in the form of an integral equation which can, in theory at least, be solved to any desired degree of accuracy by a method of successive approximations. We call such a solution 'quasi-analytic'; it is analytic in the sense that only closed-form integrals (in which the integrands are always known functions) require evaluation by quadratures, but it is non-analytic in the sense that each successive analytic calculation of this kind yields merely an improved approximation to the exact solution so that a whole series of such calculations are needed before the required level of accuracy is reached. This procedure is virtually analytic, however, when compared with a purely numerical approach in which the problem itself is first replaced by its discrete analogue with the aid of (for example) either finite difference or finite element approximations, and then the resulting large system of linear equations solved numerically.

Although the use of successive approximations is a standard way of solving certain integral equations (see e.g. Vladimirov 1984, chapter IV), it was first formulated for the solution of a problem in electromagnetic induction by Weidelt (1966), and applied to the two-plate and quarter-space problems by Klügel (1976, 1977) and to a problem in cylindrical geometry by Rodemann (1978). A slight variation of the method was also proposed independently by Mann (1970).

In this paper a considerable simplication of the required numerical integrations is achieved by some further analytical development of the method. The penalty that must be paid for this reduced dependence on integration by quadratures is the extra burden of some rather tiresome algebra which arises from the analytical evaluation of certain integrals. However, we believe that the relative simplicity of the modified method is well worth the price of the additional manipulative algebra which, in any case, only has to be done once. The modified method is established in Sections 3–6, and is then used to generate the quasi-analytic solution for E-polarization induction in the same particular control model as described in paper I. In Section 8 the results obtained are again compared with the corresponding numerical results given by (i) the finite difference program of Brewitt-Taylor & Weaver (1976) (including an improved procedure for calculating the derived fields which is described in Section 7), and (ii) the finite element program of Kisak & Silvester (1975). As in paper I the actual numerical values obtained at certain selected points both on the surface of and inside the conductor are tabulated alongside each other for ease in checking the accuracy of the two numerical programs against the quasi-analytic solution.

2 Basic equations and boundary conditions

The control model consisting of a conducting plate $0 < z < d$ divided into three regions $y < -a$, $|y| < a$ and $y > a$ of conductivities σ_1, σ_2 and σ_3 respectively, and underlain by a perfect conductor, is the same as in paper I and is reproduced here in Fig. 1 for convenient reference. Vacuum permeability μ_0 is assumed everywhere. For a quasi-static, time harmonic electromagnetic field in the E-polarization mode, the electric and magnetic vectors can be expressed in the component form

$$\mathbf{E}(y, z, t) = [U(y, z), 0, 0] \exp(i\omega t), \quad \mathbf{B}(y, z, t) = [0, Y(y, z), Z(y, z)] \exp(i\omega t),$$

where ω is sufficiently small that displacement currents can be neglected. We shall find it useful in this paper to label the three regions of the plate in the plane $x = 0$ as $\mathscr{S}_1$, $\mathscr{S}_2$ and $\mathscr{S}_3$ consecutively, from left to right and sometimes it will be helpful to distinguish between the different mathematical expressions for the field in these regions by writing

$$U = U_i, \quad Y = Y_i, \quad Z = Z_i, \quad [(y, z) \in \mathscr{S}_i, \quad i = 1, 2, 3]. \tag{1}$$

The field components in $\mathscr{S}_i$ are connected by the Maxwell equations

$$i\omega Y_i = -\partial U_i/\partial z, \quad i\omega Z_i = \partial U_i/\partial y, \quad \mu_0 \sigma_i U_i = \partial Z_i/\partial y - \partial Y_i/\partial z \tag{2}$$

from which it follows that

$$(\nabla^2 - i\kappa_i)\, U_i = 0, \tag{3}$$

where $\nabla^2 \equiv \partial^2/\partial y^2 + \partial^2/\partial z^2$ and $\kappa_i = \omega\mu_0\sigma_i$.

The usual boundary conditions specifying the continuity of the tangential electric and magnetic fields across the vertical boundaries within the conducting plate, and the vanishing of the tangential electric field at the surface of a perfect conductor can be expressed in terms of the electric component as follows:

$$U_1 = U_2, \quad \partial U_1/\partial y = \partial U_2/\partial y \text{ on } y = -a\ (0 < z < d), \tag{4}$$

$$U_2 = U_3, \quad \partial U_2/\partial y = \partial U_3/\partial y \text{ on } y = a\ (0 < z < d), \tag{5}$$

and for $i = 1, 2, 3$

$$U_i = 0 \text{ on } z = d. \tag{6}$$

As $|y| \to \infty$, the model becomes 1-D so in addition we have

$$\partial U_1/\partial y \to 0 \text{ as } y \to -\infty; \quad \partial U_3/\partial y \to 0 \text{ as } y \to +\infty. \tag{7}$$

On $z = 0$, U, Y and Z are all continuous, and as $|y| \to \infty$ in $z < 0$ the 1-D solution gives $Y \to B_0$, a constant. In the B-polarization problem discussed in paper I we were able to use

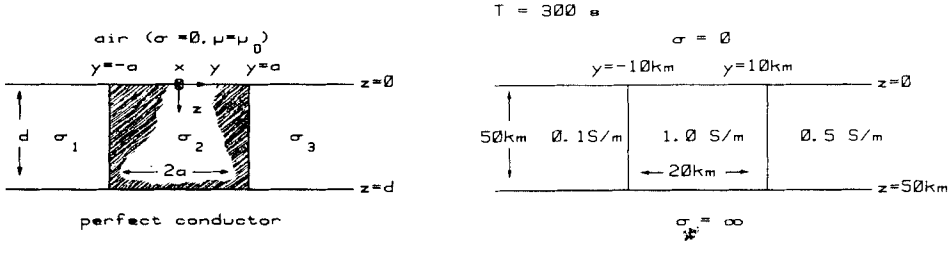

Figure 1. The control model and the parameters used in the numerical calculations.

the fact that the magnetic field was B_0 everywhere in $z < 0$ (and in particular on $z = 0$) but no such simple boundary condition exists in E-polarization. It is therefore necessary to resort to the integral relation (Schmucker 1971)

$$Y(y, 0) = B_0 - \mathscr{K} Z(y, 0), \tag{8}$$

where $\mathscr{K}$ is the Kertz operator (or negative Hilbert transform) defined by

$$\mathscr{K}\phi(y) = \frac{1}{\pi} \bar{\int}_{-\infty}^{\infty} \frac{\phi(\eta)}{y - \eta} d\eta. \tag{9}$$

The bar on the integral sign indicates the Cauchy principal value.

3 The method of successive approximations

A quasi-analytic solution of the control model will be obtained by successive approximation based on the scheme first proposed by Weidelt (1966) and subsequently applied to particular models by Klügel (1977) and Rodemann (1978). The main steps of the method will be outlined in this section with the details of the calculation left until later.

For $(y, z) \in \mathscr{S}_i$ and $(v, w) \in \mathscr{S}_j$ we seek first the Green's function $G_{ij}(y, z \mid v, w)$ which is the solution, in $\mathscr{S}_i$, of

$$(\nabla^2 - i\kappa_i)\, G_{ij}(y, z \mid v, w) = \delta(y - v)\, \delta(z - w) \tag{10}$$

that satisfies the boundary conditions

$$G_{ij}(y, d \mid v, w) = 0, \quad G'_{ij}(y, 0 \mid v, w) = 0, \tag{11}$$

where $G'_{ij} \equiv \partial G_{ij}/\partial z$. The rhs of (10) clearly vanishes in $\mathscr{S}_i$ unless (v, w) also belongs to $\mathscr{S}_i$. In addition we require the separate functions G_{1j} and G_{3j} to have vanishing gradients at infinity and to match G_{2j} smoothly across the boundaries $y = \pm a$ through the same boundary conditions (7), (4) and (5) as are satisfied by U_1, U_3 and U_2. If we now multiply (10) by U_i and (3) by G_{ij}, subtract, and then integrate over the region $\mathscr{S}_i$ using the property of the delta function we obtain

$$\iint_{\mathscr{S}_i} \{U_i(y, z)\nabla^2 G_{ij}(y, z \mid v, w) - G_{ij}(y, z \mid v, w)\nabla^2 U_i(y, z)\}\, dydz = \begin{cases} U_j(v, w) & (i = j) \\ 0 & (i \neq j). \end{cases} \tag{12}$$

The lhs of (12) can be transformed by Green's identity into a closed line integral around the boundary of $\mathscr{S}_i$, and when the three equations corresponding to $i = 1, 2, 3$ are summed the result is

$$\sum_{i=1}^{3} \oint_{\mathscr{C}_i} \left\{U_i(y, z)\, \frac{\partial G_{ij}(y, z \mid v, w)}{\partial n} - G_{ij}(y, z \mid v, w)\, \frac{\partial U_i(y, z)}{\partial n}\right\} dl_i = U_j(v, w), \tag{13}$$

where dl_i is an element of length (i.e. either dy or dz) of the rectangular contour $\mathscr{C}_i$ (the rectangles $\mathscr{C}_1$ and $\mathscr{C}_3$ actually extend to infinity) enclosing the region $\mathscr{S}_i$ and where $\partial/\partial n$ denotes the outward normal derivative (i.e. either $\pm\partial/\partial z$ or $\pm\partial/\partial y$) on this contour. The line integrals along the common segment $y = -a$ of the two contours $\mathscr{C}_1$ and $\mathscr{C}_2$ clearly cancel each other by virtue of the boundary conditions (4) satisfied by G_{1j} and G_{2j} as well as by U_1 and U_2. Likewise (5) ensures the cancellation of the integrals along $y = +a$. Finally as a result of (6), the first of conditions (11) and the fact that G_{1j} and G_{3j} also satisfy (7), the line integrals along $z = d$ and at infinity all vanish. Thus with the second of conditions (11),

equation (13) reduces to

$$\int_{-\infty}^{-a} G_{1j}(y, 0|v, w)\, U_1'(y, 0)\, dy + \int_{-a}^{a} G_{2j}(y, 0|v, w)\, U_2'(y, 0)\, dy + \int_{a}^{\infty} G_{3j}(y, 0|v, w)\, U_3'(y, 0)\, dy = U_j(v, w), \tag{14}$$

where $U_i' \equiv \partial U_i/\partial z$.

Now the reciprocity property of the Green's function requires

$$G_{ij}(y, z\,|v, w) = G_{ji}(v, w\,|y, z), \tag{15}$$

a fact which can be verified directly from the explicit expressions for G_{ij} obtained in Section 4. Thus, by interchanging the variables in (14), using (15) and the first of Maxwell's equations (2), noting the definitions in (1) and further defining for $i = 1, 2, 3$ and $j = 1, 2, 3$,

$$G(y, z, v) = G_{ij}(y, z\,|v, 0) \quad [(y, z) \in \mathscr{S}_i,\ (v, 0+) \in \mathscr{S}_j], \tag{16}$$

we may write (14) in the form

$$U(y, z) = -i\omega \int_{-\infty}^{\infty} G(y, z, v)\, Y(v, 0)\, dv \tag{17}$$

which gives the electric field everywhere in the plate $0 < z < d$. Differentiating this equation according to Maxwell's equations (2) we also obtain for $0 < z < d$

$$Y(y, z) = \int_{-\infty}^{\infty} G'(y, z, v)\, Y(v, 0)\, dv \tag{18}$$

$$Z(y, z) = -\int_{-\infty}^{\infty} \Gamma(y, z, v)\, Y(v, 0)\, dv, \tag{19}$$

where

$$\Gamma(y, z, v) = \partial G(y, z, v)/\partial y. \tag{20}$$

Substitution of (19) evaluated at $z = 0+$ in (8) gives

$$Y(y, 0) = B_0 + \mathscr{K} \int_{-\infty}^{\infty} \Gamma(y, 0, v)\, Y(v, 0)\, dv. \tag{21}$$

This leads at once to Weidelt's scheme of successive approximations. Starting with

$$Y^{[0]}(y, 0) = B_0, \tag{22}$$

which is the field that would obtain if the plate were uniform, we write, according to (21), the $(n+1)$th approximation $(n \geqslant 0)$ as

$$Y^{[n+1]}(y, 0) = B_0 + \mathscr{K} \int_{-\infty}^{\infty} \Gamma(y, 0, v)\, Y^{[n]}(v, 0)\, dv. \tag{23}$$

The surface magnetic field is then given by

$$Y(y, 0) = \lim_{N \to \infty} Y^{[N]}(y, 0) \tag{24}$$

provided that this sequence converges. Once $Y(y, 0)$ has been found the entire electromagnetic field within the plate can be found from (17), (18) and (19).

The alternative version of this scheme proposed by Mann (1970) follows immediately if we define for $n \geq 0$

$$\Delta^{[n]}(y) = Y^{[n]}(y, 0) - Y^{[n-1]}(y, 0) \tag{25}$$

so that (22) and (23) can be recast in the form

$$\Delta^{[0]}(y) = B_0 \tag{26}$$

$$\Delta^{[n+1]}(y) = \mathscr{K} \int_{-\infty}^{\infty} \Gamma(y, 0, v)\, \Delta^{(n)}(v)\, dv, \tag{27}$$

giving

$$Y(y, 0) = \sum_{N=0}^{\infty} \Delta^{[N]}(y) \tag{28}$$

provided that this series converges.

The first approximation $\Delta^{(1)}$ can actually be calculated analytically in terms of the exponential integral function. Putting $h(y) \equiv \Delta^{(1)}(y)/B_0$, substituting from (9) for the operator $\mathscr{K}$ in (27) (with $n = 0$), and interchanging the order of integration, we obtain

$$h(y) \equiv \mathscr{K} \int_{-\infty}^{\infty} \Gamma(y, 0, v)\, dv = \int_{-\infty}^{\infty} \Xi(y, v)\, dv \tag{29}$$

where

$$\Xi(y, v) = \frac{1}{\pi} \int_{-\infty}^{\infty} \frac{\Gamma(\eta, 0, v)}{y - \eta}\, d\eta. \tag{30}$$

It is the function $\Xi(y, v)$ which is expressed in terms of the exponential integral function by the formula in (30). The first approximation to the field itself is then given analytically by the expression.

$$Y^{[1]}(y, 0) = B_0 \{1 + h(y)\}. \tag{31}$$

In fact for the special cases of the two-plate model ($\sigma_2 = \sigma_3$, $y' = y + a$) and the quarter-space ($\sigma_2 = \sigma_3$, $y' = y + a$, $d \to \infty$), the expression (31) reduces to the approximate solutions calculated by Treumann (1970) and Weaver & Thomson (1972) respectively. Earlier Weaver (1963) had used the zero-th approximation (22) to obtain first approximations to the other components of the field for the quarter-space model according to the formulae (17), (18) and (19).

These results enable us to develop yet another variation of Weidelt's method in which the integration procedure is very much simplified. Interchanging the operator $\mathscr{K}$ and the integral in equation (21) with the aid of the result (30), and also adding and subtracting $h(y)\, Y(y, 0)$ on the rhs using the integral representation (29) for the subtracted term, we obtain

$$Y(y, 0) = B_0 + h(y)\, Y(y, 0) + \int_{-\infty}^{\infty} \Xi(y, v)\, \{Y(v, 0) - Y(y, 0)\}\, dv.$$

The form of this equation suggests that the $(n + 1)$th approximation can be expressed by the

formula

$$Y^{[n+1]}(y, 0) = B_0 + h(y)\, Y^{[n]}(y, 0) + \int_{-\infty}^{\infty} \Xi(y, v)\, \{Y^{[n]}(v, 0) - Y^{[n]}(y, 0)\}\, dv \qquad (32)$$

which together with (31) defines the iterative scheme that we shall use. It will be seen that $h(y)$ and $\Xi(y, v)$ can be calculated analytically from the formulae (29) and (30). This results in a considerable reduction in the amount of numerical work required; the double integral appearing in the original equation (23) is reduced to a single integral and the potentially troublesome numerical evaluation of the Hilbert transform $\mathscr{H}$ is avoided altogether. The subtraction of the magnetic fields in (32) effectively removes a logarithmic singularity in the integrand that would otherwise occur at $v = y$ through the presence of the exponential integral function in $\Xi(y, v)$.

Although each step in the iterative scheme defined by (31) and (32) requires a numerical integration by quadratures, the integrands involved are always known functions, and as stated in Section 1, it is for this reason that the solution we obtain is called 'quasi-analytic' rather than numerical. There remains, in fact, a considerable amount of analytical development to be done before the quasi-analytic solution for the control model under consideration can be obtained by the method described in this section. Included in this development is the analytic calculation of the functions G, Γ, Ξ, and h which will be dealt with in Sections 4 and 5.

4 Calculation of the Green's function

As remarked earlier the rhs of (10) vanishes except when $i = j$. Thus for $i \neq j$ the general solution of (10) satisfying the boundary conditions (11) can be expressed in the form

$$G_{ij}(y, z\,|v, w) = \frac{1}{d} \sum_{m=0}^{\infty} \{\mathscr{A}_m^{ij} \exp(\gamma_m^{(i)} y) + \mathscr{B}_m^{ij} \exp(-\gamma_m^{(i)} y)\} \cos(k_m z) \cos(k_m w) \qquad (33)$$

where

$$k_m = (2m + 1)\, \pi/2d, \quad \gamma_m^{(i)} = \sqrt{k_m^2 + i\kappa_i} \qquad (34)$$

and where $\mathscr{A}_m^{ij}$ and $\mathscr{B}_m^{ij}$ are arbitrary functions of v and w, with the factors $(1/d) \cos(k_m w)$ included with them for algebraic convenience. It is understood that

$$\mathscr{A}_m^{3j} = \mathscr{B}_m^{1j} \equiv 0 \qquad (35)$$

so that the boundary conditions at infinity corresponding to (7) may also be satisfied. The rhs of (33) will be recognized as the Fourier series expansion of G_{ij} in $0 < z < d$.

To find the remaining functions G_{ii} we first seek the solution of (10) in the entire strip $-\infty < y < \infty$, $0 < z < d$, subject to the boundary conditions (11). This will serve as a particular integral G_{ii}^* in the appropriate region $\mathscr{S}_i$. The general solution G_{ii} can then be found by adding auxiliary solutions of the form (33). Putting $i = j$ in (10) and taking its finite cosine transform defined by

$$\phi(k_m) = \int_0^d \Phi(z) \cos(k_m z)\, dz, \qquad (36)$$

we obtain after applying the boundary conditions (11) and using the property of the delta function

$$[\partial^2/\partial y^2 - (\gamma_m^{(i)})^2]\, g_{ii}(y, k_m\,|v, w) = \delta(y - v) \cos(k_m w). \qquad (37)$$

If the exponential Fourier transform defined by

$$\hat{\phi}(\eta) = \frac{1}{\sqrt{2\pi}} \int_{-\infty}^{\infty} \phi(y) \exp(i\eta y)\, dy$$

is now applied to (37), then we obtain

$$\hat{g}_{ii}(\eta, k_m | v, w) = -\frac{\exp(i\eta v)\cos(k_m w)}{\sqrt{2\pi}[\eta^2 + (\gamma_m^{(i)})^2]}$$

whose inverse is

$$g_{ii}(y, k_m | v, w) = -\frac{\cos(k_m w)}{2\pi} \int_{-\infty}^{\infty} \frac{\exp[i\eta(v-y)]}{\eta^2 + (\gamma_m^{(i)})^2}\, d\eta$$

$$= -\frac{\exp(-\gamma_m^{(i)}|y - v|)}{2\gamma_m^{(i)}} \cos(k_m w). \tag{38}$$

Finally, it follows from the well-known formula for the coefficients of a Fourier cosine series (or by Sneddon 1951, p. 73) that the inverse of (36) is

$$\Phi(z) = \frac{2}{d} \sum_{m=0}^{\infty} \phi(k_m) \cos(k_m z),$$

so that by inverting (38) we find that the particular integral in $\mathscr{S}_i$ is

$$G_{ii}^*(y, z | v, w) = -\frac{1}{d} \sum_{m=0}^{\infty} \frac{\exp(-\gamma_m^{(i)}|y - v|)}{\gamma_m^{(i)}} \cos(k_m z)\cos(k_m w). \tag{39}$$

By (16), (33) and (39) it is now clear that the required form of the Green's function is

$$G(y, z, v) = \frac{1}{d} \sum_{m=0}^{\infty} \bar{G}_{ij}(y, v)\cos(k_m z) \quad [(y, z) \in \mathscr{S}_i, (v, 0+) \in \mathscr{S}_j], \tag{40}$$

with

$$\bar{G}_{ij}(y, v) = \mathscr{A}_m^{ij} \exp(\gamma_m^{(i)} y) + \mathscr{B}_m^{ij} \exp(-\gamma_m^{(i)} y) - \delta_{ij} \exp(-\gamma_m^{(j)}|y - v|)/\gamma_m^{(j)}, \tag{41}$$

where δ_{ij} is the Kronecker delta. Bearing in mind the definitions (36), we see that there are 12 non-vanishing coefficients $\mathscr{A}_m^{ij}$ and $\mathscr{B}_m^{ij}$ for each m. These can be determined from the 12 boundary conditions (corresponding to (4) and (5)) which prescribe the smooth matching of G_{1j} and G_{2j} across $y = -a$ and G_{2j} and G_{3j} across $y = +a$. This is clearly a straightforward but tedious algebraic exercise. Here we quote only the final expressions for $\bar{G}_{ij}$; it can easily be verified directly that they satisfy the required boundary conditions.

First it is necessary to introduce some simplifying notation. In the following it is understood that l can take the values 1 or 3. Introducing the parameters

$$\alpha_m^{(l)} = \gamma_m^{(l)} + \gamma_m^{(2)},\ \beta_m^{(l)} = \gamma_m^{(l)} - \gamma_m^{(2)},\ \lambda_m^{(l)} = \chi_m^{(l)} + \gamma_m^{(2)},\ \nu_m^{(l)} = \chi_m^{(l)} - \gamma_m^{(2)} \tag{42}$$

where

$$\chi_m^{(l)} = \gamma_m^{(l)}\gamma_m^{(3)}/\gamma_m^{(l)}, \tag{43}$$

we define the functions

$$r_m^{(I)}(\xi, \eta) = \lambda_m^{(I)} \exp\left[-(\xi - \eta)\gamma_m^{(2)}\right] + \nu_m^{(I)} \exp\left[-(\xi + \eta + 2a)\gamma_m^{(2)}\right] \tag{44}$$

$$s_m^{(I)}(\xi, \eta) = \lambda_m^{(I)} \exp\left[-(\xi - \eta)\gamma_m^{(2)}\right] - \nu_m^{(I)} \exp\left[-(\xi + \eta + 2a)\gamma_m^{(2)}\right], \tag{45}$$

and also

$$A_m^{(I)}(\xi, \eta) = D_m\left[2\nu_m^{(I)} \exp(-4a\gamma_m^{(2)}) - (\beta_m^{(I)}/\gamma_m^{(I)})\, r_m^{(I)}(a, a)\right] \exp\left[(2a - \xi - \eta)\gamma_m^{(I)}\right] \tag{46}$$

$$C_m^{(I)}(\xi, \eta) = (\beta_m^{(I)} D_m/\gamma_m^{(2)})\, s_m^{(I)}(\xi, \eta) \exp(-2a\gamma_m^{(2)}) \tag{47}$$

$$\begin{aligned} L_m^{\pm(I)}(\xi, \eta) = D_m \big[\!\big[& 2\lambda_m^{(I)} \{1 - \exp[(a - \eta)\beta_m^{(I)}]\} + (\beta_m^{(I)}/\gamma_m^{(2)})\, s_m^{(I)}(a, a) \\ & \pm 2\nu_m^{(I)} \exp[(a - \eta)\beta_m^{(I)} - 2(a + \xi)\gamma_m^{(2)}]\big]\!\big] \exp\left[(\xi - \eta)\gamma_m^{(2)}\right] \end{aligned} \tag{48}$$

$$M_m^{(I)}(\xi, \eta) = -4\gamma_m^{(2)} D_m \exp_{+}^{\sim}\left[(a - \xi)\gamma_m^{(I)} + (a - \eta)\chi_m^{(I)} - 2a\gamma_m^{(2)}\right] \tag{49}$$

$$\begin{aligned} N_m^{(I)}(\xi, \eta) = D_m \big[\!\big[& 2\lambda_m^{(I)} \{1 - \exp[(a - \eta)\beta_m^{(I)}]\} - (\beta_m^{(I)}/\gamma_m^{(I)})\, r_m^{(I)}(a, a) \\ & + 2\nu_m^{(I)} \exp[(a - \eta)\alpha_m^{(I)} - 4a\gamma_m^{(2)}]\big]\!\big] \exp\left[(\eta - \xi)\gamma_m^{(I)}\right], \end{aligned} \tag{50}$$

where we have written

$$D_m = [\alpha_m^{(1)} \alpha_m^{(3)} - \beta_m^{(1)} \beta_m^{(3)} \exp(-4a\gamma_m^{(2)})]^{-1}. \tag{51}$$

The required formulae for $\bar{G}_{ij}$ are

$$\begin{aligned} \bar{G}_{11}(y, v) &= A_m^{(1)}(-y, -v) - (\gamma_m^{(1)})^{-1} \exp(-|y - v|\gamma_m^{(1)}) \\ \bar{G}_{22}(y, v) &= C_m^{(1)}(y, -v) + C_m^{(3)}(-y, v) - (\gamma_m^{(2)})^{-1} \exp(-|y - v|\gamma_m^{(2)}) \\ \bar{G}_{33}(y, v) &= A_m^{(3)}(y, v) - (\gamma_m^{(3)})^{-1} \exp(-|y - v|\gamma_m^{(3)}) \\ \bar{G}_{12}(y, v) &= N_m^{(1)}(-y, -v) - (\gamma_m^{(1)})^{-1} \exp[(y - v)\gamma_m^{(1)}] \\ \bar{G}_{21}(y, v) &= L_m^{+(1)}(-y, -v) - (\gamma_m^{(2)})^{-1} \exp[(v - y)\gamma_m^{(2)}] \\ \bar{G}_{23}(y, v) &= L_m^{+(3)}(y, v) - (\gamma_m^{(2)})^{-1} \exp[(y - v)\gamma_m^{(2)}] \\ \bar{G}_{32}(y, v) &= N_m^{(3)}(y, v) - (\gamma_m^{(3)})^{-1} \exp[(v - y)\gamma_m^{(3)}] \\ \bar{G}_{13}(y, v) &= M_m^{(1)}(-y, v), \quad \bar{G}_{31}(y, v) = M_m^{(3)}(y, -v). \end{aligned} \tag{52}$$

The derived Green's function entering (18) is obtained from (40) in the form

$$G'(y, z, v) = -\frac{1}{d} \sum_{m=0}^{\infty} k_m \bar{G}_{ij}(y, v) \sin(k_m z) \quad [(y, z) \in \mathscr{S}_i,\ (v, 0+) \in \mathscr{S}_j], \tag{53}$$

where the $\bar{G}_{ij}$ are given by (52). The function Γ defined in (20) can be found by differentiating the expressions (52) with respect to y. Writing

$$\Gamma(y, z, v) = \frac{1}{d} \sum_{m=0}^{\infty} \bar{\Gamma}_{ij}(y, v) \cos(k_m z) \quad [(y, z) \in \mathscr{S}_i,\ (v, 0+) \in \mathscr{S}_j] \tag{54}$$

it follows at once that

$$\begin{aligned}
\bar{\Gamma}_{11}(y, v) &= \gamma_m^{(1)} A_m^{(1)}(-y, -v) + \operatorname{sgn}(y - v) \exp(-|y - v|\gamma_m^{(1)}) \\
\bar{\Gamma}_{22}(y, v) &= -\gamma_m^{(2)} C_m^{(1)}(y, -v) + \gamma_m^{(2)} C_m^{(3)}(-y, v) + \operatorname{sgn}(y - v) \exp(-|y - v|\gamma_m^{(2)}) \\
\bar{\Gamma}_{33}(y, v) &= -\gamma_m^{(3)} A_m^{(3)}(y, v) + \operatorname{sgn}(y - v) \exp(-|y - v|\gamma_m^{(3)}) \\
\bar{\Gamma}_{12}(y, v) &= \gamma_m^{(1)} N_m^{(1)}(-y, -v) - \exp[(y - v)\gamma_m^{(1)}] \\
\bar{\Gamma}_{21}(y, v) &= -\gamma_m^{(2)} L_m^{-(1)}(-y, -v) + \exp[(v - y)\gamma_m^{(2)}] \\
\bar{\Gamma}_{23}(y, v) &= \gamma_m^{(2)} L_m^{-(3)}(y, v) - \exp[(y - v)\gamma_m^{(2)}] \\
\bar{\Gamma}_{32}(y, v) &= -\gamma_m^{(3)} N_m^{(3)}(y, v) + \exp[(v - y)\gamma_m^{(3)}] \\
\bar{\Gamma}_{13}(y, v) &= \gamma_m^{(1)} M_m^{(1)}(-y, v), \qquad \bar{\Gamma}_{31}(y, v) = -\gamma_m^{(3)} M_m^{(3)}(y, -v).
\end{aligned} \tag{55}$$

It can be seen from (34) and (42) that

$$\beta_m^{(l)} \equiv i(\kappa_l - \kappa_2)/\alpha_m^{(l)}$$

whence all coefficients of those exponential functions in (46)–(50) that reduce to unity when $y = v = \pm a$ are $O(1/k_m^3)$ for large m. (In this regard note that the first terms in the expressions for $L_m^{\pm(l)}$ and $N_m^{(l)}$ vanish at these points.) This property is important since it ensures that the associated terms in (55) are $O(1/k_m^2)$ thereby guaranteeing the convergence of their contributions to the infinite series (54) at $v = y = \pm a$. The final terms in the expressions (55) give rise to a singularity in Γ at $v = y$. This is discussed in more detail in Section 6.

5 Calculation of the functions Ξ and h

It was remarked in Section 2 that the function $\Xi(y, v)$ can be evaluated in terms of the exponential integral function which is defined by the formula (Gautschi & Cahill, 1964)

$$E_1(\zeta) = \int_\zeta^\infty \frac{e^{-u}}{u} \qquad (|\arg \zeta| < \pi). \tag{56}$$

The analytic properties of the function which we shall need to use are exhibited by its series expansion

$$E_1(\zeta) = -C - \log \zeta - \sum_{n=1}^{\infty} \frac{(-1)^n \zeta^n}{n\, n!} \tag{57}$$

(C is Euler's constant) and by its asymptotic representation as $\zeta \to \infty$

$$E_1(\zeta) \sim (e^{-\zeta}/\zeta)(1 - 1/\zeta). \tag{58}$$

Now from the definitions (29), (30) and (54) we note that if we write

$$\Xi(y, v) = \Xi_j(y, v) \qquad [(v, 0+) \in \mathscr{S}_j] \tag{59}$$

then

$$h(y) = \int_{-\infty}^{-a} \Xi_1(y, v)\, dv + \int_{-a}^{a} \Xi_2(y, v)\, dv + \int_a^\infty \Xi_3(y, v)\, dv \tag{60}$$

where for $j = 1, 2, 3$

$$\Xi_j(y, v) = \frac{1}{\pi d} \sum_{m=0}^{\infty} \left\{ \int_{-\infty}^{-a} \frac{\bar{\Gamma}_{1j}(\eta, v)}{y - \eta} d\eta + \int_{-a}^{a} \frac{\bar{\Gamma}_{2j}(\eta, v)}{y - \eta} d\eta + \int_{a}^{\infty} \frac{\bar{\Gamma}_{3j}(\eta, v)}{y - \eta} d\eta \right\}. \quad (61)$$

Actually only one of the three integrals in (61) has a singularity at $y = \eta$ for any given value of y. For example, if $y > a$ then only the third integral need be calculated as a Cauchy principal value. In fact by examining the formulae (55) giving $\bar{\Gamma}_{31}$, $\bar{\Gamma}_{32}$ and $\bar{\Gamma}_{33}$ and the associated definitions (46), (47) and (48) we see that the third term in (61) involves integrals of just two types, namely

$$I_3 = \int_a^{\infty} \frac{\exp(-\eta\gamma)}{y - \eta} d\eta, \quad J_3 = \int_a^{\infty} \operatorname{sgn}(\eta - v) \frac{\exp(-|\eta - v|\gamma)}{y - \eta} d\eta \quad (v > a).$$

Here we have temporarily written γ instead of $\gamma_m^{(3)}$. The transformation $s = (\eta - y)\gamma$ yields

$$I_3 = -\exp(-y\gamma) \int_{\zeta_0}^{\infty} \frac{e^{-s}}{s} ds, \quad (62)$$

where $\zeta_0 = (a - y)\gamma$. The path of integration $\mathscr{C}$ in the complex s-plane runs from $|s| = |\zeta_0|$ to $|s| = \infty$ along the radial line $\arg s = \arg \zeta_0$. When $y < a$, ζ_0 lies in the first quadrant of the s-plane and the integral in (62) is just $E_1(\zeta_0)$ as defined in (56). But when $y > a$, ζ_0 is in the third quadrant and $\mathscr{C}$ passes through the pole at $s = 0$ where the Cauchy principal value of the integral must be taken. However, if the contour is indented around the pole along a semi-circle $\mathscr{C}_0$ of vanishingly small radius, as shown in Fig. 2, then the integral along $\mathscr{C} + \mathscr{C}_0$ still gives $E_1(\zeta_0)$ according to the definition (56). Since the residue at $s = 0$ is 1 the contribution from $\mathscr{C}_0$ is πi and we deduce that for all y

$$I_3 = -\exp(-y\gamma) \{E_1(\zeta_0) - \pi i H(y - a)\}, \quad (63)$$

where $H(y)$ is the Heaviside function equal to 1 for $y > 0$ and 0 for $y < 0$. The integral J_3 can be similarly transformed and rearranged to give

$$J_3 = e^{-\zeta_1} \left\{ \int_{-\zeta_0}^{\infty} \frac{e^{-s}}{s} ds - \int_{-\zeta'}^{\infty} \frac{e^{-s}}{s} ds \right\} - e^{\zeta'} \int_{\zeta'}^{\infty} \frac{e^{-s}}{s} ds \quad (v > a),$$

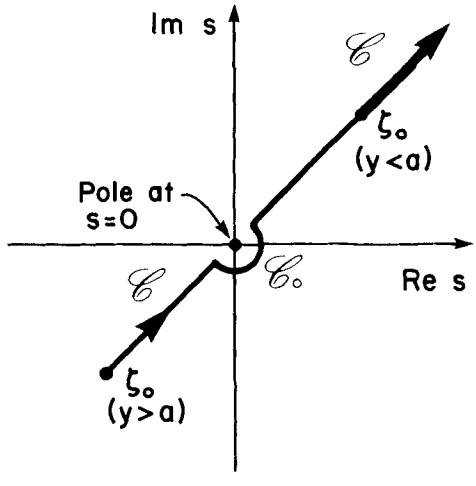

Figure 2. The contours $\mathscr{C}$ and $\mathscr{C}_0$ in the complex s-plane.

where $\zeta' = (v - y)\gamma$. These integrals are all of the type (62) and can therefore be evaluated as in (63). After some further manipulation of the Heaviside functions (recalling that $v > a$) we finally obtain

$$J_3 = e^{-\zeta'}\{E_1(-\zeta_0) - E_1(-\zeta')\} - e^{\zeta'}E_1(\zeta') + \pi i H(y-a)\exp(-|y-v|\gamma).$$

Similarly, integrals of the type

$$I_1 = \int_{-\infty}^{-a} \frac{\exp(\eta\gamma)}{y-\eta}\,d\eta, \quad J_1 = \int_{-\infty}^{-a} \operatorname{sgn}(\eta - v)\,\frac{\exp(-|\eta - v|\gamma)}{y-\eta}\,d\eta \quad (v < -a)$$

and

$$I_2^{\pm} = \int_{-a}^{a} \frac{\exp(\pm\eta\gamma)}{y-\eta}\,d\eta, \quad J_2 = \int_{-a}^{a} \operatorname{sgn}(\eta - v)\,\frac{\exp(-|\eta - v|\gamma)}{y-\eta}\,d\eta \quad (|v| < a)$$

arise from the formulae (55) for $\bar{\Gamma}_{11}$, $\bar{\Gamma}_{12}$, $\bar{\Gamma}_{13}$ and $\bar{\Gamma}_{21}$, $\bar{\Gamma}_{22}$, $\bar{\Gamma}_{23}$ respectively and can be calculated in like manner. Introducing the functions

$$f(\zeta) = e^{\zeta}E_1(\zeta), \quad g(\zeta) = f(\zeta) + f(-\zeta), \tag{64}$$

we can summarise all the results as follows:

$$I_{1,3} = \pm\exp(-a\gamma)\,f[(a \pm y)\gamma] \mp \pi i H(\mp y - a)\exp(\pm y\gamma) \tag{65}$$

$$J_{1,3} = -g[(v-y)\gamma] + \exp[(a \pm v)\gamma]\,f[(\mp y - a)\gamma] + \pi i H(\mp y - a)\exp(-|v-y|\gamma) \tag{66}$$

$$I_2^{\pm} = \exp(\pm a\gamma)\,f[\pm(y-a)\gamma] - \exp(\mp a\gamma)\,f[\pm(y+a)\gamma] \mp \pi i H(a-|y|)\exp(\pm y\gamma) \tag{67}$$

$$J_2 = -g[(v-y)\gamma] + \exp[-(a+v)\gamma]\,f[(a+y)\gamma] + \exp[-(a-v)\gamma]\,f[(a-y)\gamma] + \pi i H(a-|y|)\exp(-|v-y|\gamma). \tag{68}$$

In (65) and (66) the upper and lower signs on the right correspond to the subscripts 1 and 3, respectively, on the left. It is clear from all these results that the final expressions for the function Ξ_j defined by (61) will be extremely complicated. After some tedious algebraic manipulation they can be written in the reasonably compact form

$$\Xi_1(y,v) = \frac{1}{\pi d}\sum_{m=0}^{\infty} [\![S_m^{(1)}(-y)\exp[(a+v)\gamma_m^{(1)}] - g[(v-y)\gamma_m^{(1)}] + \pi i H(-y-a)\{\exp(-|v-y|\gamma_m^{(1)}) - \exp(-|v+y+2a|\gamma_m^{(1)})\}]\!] \tag{69}$$

$$\Xi_2(y,v) = \frac{1}{\pi d}\sum_{m=0}^{\infty} \{T_m^{(1)}(-y,-v) + T_m^{(3)}(y,v) - g[(v-y)\gamma_m^{(2)}] + \pi i H(a-|y|)\exp(-|v-y|\gamma_m^{(2)})\} \tag{70}$$

$$\Xi_3(y,v) = \frac{1}{\pi d}\sum_{m=0}^{\infty} [\![S_m^{(3)}(y)\exp[(a-v)\gamma_m^{(3)}] - g[(v-y)\gamma_m^{(3)}] + \pi i H(y-a)\{\exp(-|v-y|\gamma_m^{(3)}) - \exp(-|v+y-2a|\gamma_m^{(3)})\}]\!] , \tag{71}$$

where we have defined for $l = 1, 3$

$$S_m^{(l)}(y) = g[(y - a)\gamma_m^{(l)}] - 2D_m\gamma_m^{(l)}s_m^{(l)}(a, a)\, f[(a - y)\gamma_m^{(l)}]$$
$$- 2\gamma_m^{(2)}D_m[\![q_m^{(l)}(-a, y) + \{2\chi_m^{(l)} f[(a + y)\chi_m^{(l)}] - q_m^{(l)}(a, y)\} \exp(-2a\gamma_m^{(2)})]\!]$$
$$+ 2\pi i D_m[\![2\gamma_m^{(2)}\chi_m^{(l)}H(-y - a) \exp[(a + y)\chi_m^{(l)} - 2a\gamma_m^{(2)}] + \gamma_m^{(2)}s_m^{(l)}(a, y)\, H(a - |y|)$$
$$+ \gamma_m^{(l)}s_m^{(l)}(a, a)\, H(y - a) \exp[(a - y)\gamma_m^{(l)}]]\!] \tag{72}$$

$$T_m^{(l)}(y, v) = D_m[\![[\alpha_m^{(l)}q_m^{(l)}(a, y) + v_m^{(l)}p_m^{(l)}(-a, -y)] \exp[-(a + v)\gamma_m^{(2)}]$$
$$- 2\gamma_m^{(l)}s_m^{(l)}(a, v) f[(a - y)\gamma_m^{(l)}] + \pi i\{2\gamma_m^{(l)}s_m^{(l)}(a, v)\, H(y - a) \exp[(a - y)\gamma_m^{(l)}]$$
$$- \beta_m^{(l)}s_m^{(l)}(-y, v)\, H(a - |y|) \exp(-2a\gamma_m^{(2)})\}]\!]. \tag{73}$$

In these expressions we have introduced the functions

$$p_m^{(l)}(\xi, \eta) = \alpha_m^{(l)} f[(\xi + \eta)\gamma_m^{(2)}] - \beta_m^{(l)} f[(\xi - \eta)\gamma_m^{(2)}] \exp(-2a\gamma_m^{(2)})$$
$$q_m^{(l)}(\xi, \eta) = \lambda_m^{(l)} f[(\xi + \eta)\gamma_m^{(2)}] - v_m^{(l)} f[(\xi - \eta)\gamma_m^{(2)}] \exp(-2a\gamma_m^{(2)}), \tag{74}$$

where, by (42) and (43),

$$p_m^{(1)}(\xi, \eta) = q_m^{(3)}(\xi, \eta), \quad p_m^{(3)}(\xi, \eta) = q_m^{(1)}(\xi, \eta).$$

For convenience in computing, note that the asymptotic form (58) shows that if we write

$$\sum_{m=0}^{\infty} g(c\gamma_m) \equiv -\frac{d^2}{c^2} + \sum_{m=0}^{\infty}\left[g(c\gamma_m) + \frac{2}{(ck_m)^2}\right], \tag{75}$$

where c represents any length, then the numerical summations of the g functions in the expressions above will converge much faster. The first term in the identity (75) follows from a well-known series

$$\sum_{m=0}^{\infty} \frac{1}{(2m + 1)^2} = \frac{\pi^2}{8} \tag{76}$$

(see e.g. Dwight 1961, 48.12). It is apparent that the expressions (69)–(71) are undefined at $v = y$ (because Ξ has a logarithmic singularity there), but this does not matter since the integrand in (32) vanishes identically at this point. This completes the calculation of $\Xi(v, y)$ in terms of tabulated functions.

Fortunately the integrations required to obtain $h(y)$ as given by (60) are relatively straightforward. All the terms except $g[(v - y)\gamma]$ in (69), (70) and (71) depend on v through simple exponential functions which can be integrated by inspection. To integrate g we first consider the integral

$$\int_b^c g[(v - y)\gamma]\, dv = \frac{1}{\gamma}\int_{\zeta_1}^{\zeta_2} e^s E_1(s)\, ds - \frac{1}{\gamma}\int_{-\zeta_1}^{-\zeta_2} e^s E_1(s)\, ds \tag{77}$$

where $\zeta_1 = (b - y)\gamma$ and $\zeta_2 = (c - y)\gamma$. The integrand is analytic on any contour joining ζ_1 and ζ_2 that does not cross the negative real axis in the complex s-plane. An integration by

parts and the fact that differentiation of (56) gives $E_1'(s) = -e^{-s}/s$ leads to the result

$$\int_{\pm\zeta_1}^{\pm\zeta_2} e^s E_1(s)\,ds = f(\pm\zeta_2) - f(\pm\zeta_1) + \log(\pm\zeta_2) - \log(\pm\zeta_1).$$

From the definitions of ζ_1 and ζ_2 we see that if $y < b < c$ or $b < c < y$ then $\arg(\pm\zeta_2) = \arg(\pm\zeta_1)$, but if $b < y < c$ then $\arg(\pm\zeta_2) = \pi \pm \arg(\pm\zeta_1)$. Hence,

$$\log(\pm\zeta_2) - \log(\pm\zeta_1) = \log|\zeta_2/\zeta_1| \pm \pi i[H(y-b) - H(y-c)]$$

and (77) can be written

$$\gamma\int_b^c g[(v-y)\gamma]\,dv = f(\zeta_2) - f(\zeta_1) - f(-\zeta_2) + f(-\zeta_1) + 2\pi i[H(y-b) - H(y-c)]. \quad (78)$$

Setting (i) $b = a$, $c = \infty$ (ii) $b = -\infty$, $c = -a$ and (iii) $b = -a$, $c = a$ and noting by (58) and (64) that $f(\pm\zeta) \to 0$ as $\zeta \to \infty$, we obtain the required integrations as follows:

$$\gamma\int_a^\infty g[(v-y)\gamma]\,dv = f[(y-a)\gamma] - f[(a-y)\gamma] + 2\pi i H(y-a) \quad (79)$$

$$\gamma\int_{-\infty}^{-a} g[(v-y)\gamma]\,dv = f[-(y+a)\gamma] - f[(y+a)\gamma] + 2\pi i H(-y-a) \quad (80)$$

$$\gamma\int_{-a}^{a} g[(v-y)\gamma]\,dv = f[(a-y)\gamma] + f[(y+a)\gamma] - f[(y-a)\gamma] - f[-(y+a)\gamma] + 2\pi i H(a-|y|). \quad (81)$$

The final expression for $h(y)$ follows after some further algebraic manipulation. We can express it quite simply as

$$h(y) = \frac{2}{\pi d}\sum_{m=0}^{\infty}[R_m^{(1)}(-y) + R_m^{(3)}(y)] \quad (82)$$

in terms of the function

$$R_m^{(l)}(y) = P_m^{(l)} f[(a-y)\gamma_m^{(l)}] - Q_m^{(l)} f[(a-y)\gamma_m^{(2)}] + \{Q_m^{(l)} - P_m^{(l)}\} f[(y-a)\gamma_m^{(2)}] - \pi i\{P_m^{(l)} H(y-a)\exp[(a-y)\gamma_m^{(l)}] + Q_m^{(l)} H(a-|y|)\exp[(a-y)\gamma_m^{(2)}]\} \quad (83)$$

in which we have defined for $l = 1, 3$

$$P_m^{(l)} = Q_m^{(l)} - (Q_m^{(l)} Q_m^{(3)}/Q_m^{(l)})\exp(2a\gamma_m^{(2)}) \quad (84)$$

$$Q_m^{(l)} = (\alpha_m^{(l)}\,\upsilon_m^{(l)}\,D_m/\gamma_m^{(2)})\,[\lambda_m^{(l)}/\chi_m^{(l)} - (\beta_m^{(l)}/\gamma_m^{(l)})\exp(-2a\gamma_m^{(2)})]\exp(-2a\gamma_m^{(2)}). \quad (85)$$

Some minor computational difficulties arise at $y = \pm a$ because of the logarithmic singularities in the functions f at these points. In fact by (57) and (64) it is readily shown that as $y \to a$

$$f[(y-a)\gamma] \sim -C - \log(|y-a|\gamma) + \pi i H(a-y). \quad (86)$$

However, these singularities cancel out in the expression for $R_m^{(1)}(y)$ above. Thus, using (86) in (83) we see that as $y \to a$

$$R_m^{(3)}(y) \sim P_m^{(3)} \log(\gamma_m^{(2)}/\gamma_m^{(3)}) - \pi i[P_m^{(3)} H(a-y) + Q_m^{(3)} H(y-a)].$$

This gives the limiting values

$$R_m^{(3)}(a+0) = P_m^{(3)} \log(\gamma_m^{(2)}/\gamma_m^{(3)}) - \pi i Q_m^{(3)}, \tag{87}$$

$$R_m^{(3)}(a-0) = P_m^{(3)} [\log(\gamma_m^{(2)}/\gamma_m^{(3)}) - \pi i].$$

There is no singularity in $R_m^{(1)}(-y)$ at $y = a$ and substitution in (83) yields

$$R_m^{(1)}(-a-0) - R_m^{(1)}(-a+0) = \pi i Q_m^{(1)} \exp(2a\gamma_m^{(2)}). \tag{88}$$

It follows from (87) and (88) that

$$R_m^{(1)}(-a-0) + R_m^{(3)}(-a+0) = R_m^{(1)}(-a+0) + R_m^{(3)}(a-0) + \pi i[P_m^{(3)} - Q_m^{(3)} + Q_m^{(1)} \exp(2a\gamma_m^{(2)})]$$

and the vanishing of the last term by virtue of (84) with $l = 3$ ensures that $h(a+0) = h(a-0) = h(a)$ where by (83) and (87)

$$h(a) = \frac{2}{\pi d} \sum_{m=0}^{\infty} [P_m^{(1)} f(2a\gamma_m^{(1)}) - Q_m^{(1)} f(2a\gamma_m^{(2)}) + (Q_m^{(1)} - P_m^{(1)}) f(-2a\gamma_m^{(2)}) + P_m^{(3)} \log(\gamma_m^{(2)}/\gamma_m^{(3)}) - \pi i Q_m^{(3)}]. \tag{89}$$

A similar discussion of the behaviour of the functions at $y = -a$ shows that

$$h(-a) = \frac{2}{\pi d} \sum_{m=0}^{\infty} [P_m^{(3)} f(2a\gamma_m^{(3)}) - Q_m^{(3)} f(2a\gamma_m^{(2)}) + (Q_m^{(3)} - P_m^{(3)}) f(-2a\gamma_m^{(2)}) + P_m^{(1)} \log(\gamma_m^{(2)}/\gamma_m^{(1)}) - \pi i Q_m^{(1)}]. \tag{90}$$

Both (89) and (90) are in a form readily amenable to computation.

Logarithmic singularities at $y = \pm a$ are also present in the functions f occurring in $S_m^{(l)}(y)$ and $T_m^{(l)}(y, v)$ defined in (72) and (73). A careful analysis again shows that they disappear when all the terms are collected together. We shall not go through the detailed arguments here which are similar to those above. However, the limiting forms of the various expressions are quoted below since these are needed for numerical computation. We have first

$$S_m^{(l)}(a) = 2\gamma_m^{(2)} D_m \{[\lambda_m^{(l)} f(2a\gamma_m^{(2)}) + v_m^{(l)} f(-2a\gamma_m^{(2)}) - 2\chi_m^{(l)} f(2a\chi_m^{(l)})] \exp(-2a\gamma_m^{(2)}) + r_m^{(l)}(a, a) \log(\gamma_m^{(2)}/\gamma_m^{(l)})\} + \pi i \alpha_m^{(l)} D_m s_m^{(l)}(a, a) \tag{91}$$

$$S_m^{(l)}(-a) = g(-2a\gamma_m^{(l)}) - 2\gamma_m^{(l)} D_m s_m^{(l)}(a, a) f(2a\gamma_m^{(l)}) - 2\gamma_m^{(2)} D_m \{\lambda_m^{(l)} f(-2a\gamma_m^{(2)}) + v_m^{(l)} f(2a\gamma_m^{(2)}) \exp(-4a\gamma_m^{(2)}) + [2\chi_m^{(l)} \log(\gamma_m^{(2)}/\chi_m^{(l)}) - \pi i \lambda_m^{(l)}] \exp(-2a\gamma_m^{(2)})\} \tag{92}$$

which when substituted in (69) and (71) give

$$\Xi_1(\pm a, v) = \frac{1}{\pi d} \sum_{m=0}^{\infty} \{S_m^{(1)}(\mp a) \exp[(a + v)\gamma_m^{(1)}] - g[(v \mp a)\gamma_m^{(1)}]\} \tag{93}$$

$$\Xi_3(\pm a, v) = \frac{1}{\pi d} \sum_{m=0}^{\infty} \{S_m^{(3)}(\pm a) \exp[(a - v)\gamma_m^{(3)}] - g[(v \mp a)\gamma_m^{(3)}]\} . \tag{94}$$

Finally, when the functions $T_m^{(l)}$ are combined with the term involving the Heaviside function in (70), it is found that unique limits of the total expression exist as $y \to \pm a$ from left or right, giving

$$\begin{aligned}\Xi_2(a, v) = \frac{1}{\pi d} \sum_{m=0}^{\infty} \{ & D_m s_m^{(3)}(a, v) [\pi i \alpha_m^{(3)} - 2\gamma_m^{(3)} \log(\gamma_m^{(2)}/\gamma_m^{(3)})] \\ & + D_m s_m^{(1)}(a, -v) [\alpha_m^{(1)} f(2a\gamma_m^{(2)}) + \beta_m^{(1)} f(-2a\gamma_m^{(2)}) - 2\gamma_m^{(1)} f(2a\gamma_m^{(1)})] \\ & - g[(v - a)\gamma_m^{(2)}]\},\end{aligned} \tag{95}$$

$$\begin{aligned}\Xi_2(-a, v) = \frac{1}{\pi d} \sum_{m=0}^{\infty} \{ & D_m s_m^{(1)}(a, -v) [\pi i \alpha_m^{(1)} - 2\gamma_m^{(1)} \log(\gamma_m^{(2)}/\gamma_m^{(1)}) \\ & + D_m s_m^{(3)}(a, v) [\alpha_m^{(3)} f(2a\gamma_m^{(2)}) + \beta_m^{(3)} f(-2a\gamma_m^{(2)}) - 2\gamma_m^{(3)} f(2a\gamma_m^{(3)})] \\ & - g[(v + a)\gamma_m^{(2)}]\}.\end{aligned} \tag{96}$$

6 Calculation of other field components

Although algebraically complicated, the functions Ξ and h required in the application of the successive approximation scheme defined by (31) and (32) are readily evaluated on the computer. Once the solution $Y(y, 0)$ has been found it is necessary to calculate the Green's functions G and Γ in order to obtain the other field components U and Z, and also Y inside the conductor, given by the integral formulae (17)–(19). There are some numerical difficulties associated with the functions $\bar{G}_{ii}$ and $\bar{\Gamma}_{ii}$ defined in (52) and (55) because they contain terms $(\gamma_m^{(i)})^{-1} \exp(-|y - v|\gamma_m^{(i)})$ and $\operatorname{sgn}(y - v) \exp(-|y - v|\gamma_m^{(i)})$ respectively which make the series (40), (53) and (54) defining G, G' and Γ quite slowly convergent near $v = y$. Moreover, at the point $v = y$ itself where the Green's functions are discontinuous, these terms cause the series to be formally divergent, although the singularities are of course integrable. Nevertheless, such behaviour makes the numerical evaluation of the Green's functions quite tricky in the neighbourhood of their discontinuities.

The singular behaviour at $v = y$ can be dealt with by noting that for $b < y < c$

$$\int_b^c \exp(-|y - v|\gamma)\, dv = \frac{1}{\gamma} \{2 - \exp[(b - y)\gamma] - \exp[(y - c)\gamma]\} \tag{97}$$

$$\int_b^c \operatorname{sgn}(y - v) \exp(-|y - v|\gamma)\, dv = \frac{1}{\gamma} \{\exp[(y - c)\gamma] - \exp[(b - y)\gamma]\} \tag{98}$$

so that for $0 < z < d$

$$\int_b^c \left[\sum_{m=0}^{\infty} \frac{\exp(-|y-v|\gamma_m^{(i)})}{\gamma_m^{(i)}} \cos(k_m z)\right] Y(v,0)\,dv$$

$$= \int_b^c \Lambda_c^{(i)}(|y-v|, z)\,[Y(v,0) - Y(y,0)]\,dv + Y(y,0)\left\{d(d-z)\right.$$

$$\left. - \sum_{m=0}^{\infty} \frac{\cos(k_m z)}{(\gamma_m^{(i)})^2} \left[\left[\frac{2i\kappa_i}{k_m^2} + \exp[(b-y)\gamma_m^{(i)}] + \exp[(y-c)\gamma_m^{(i)}]\right]\right)\right., \tag{99}$$

$$\int_b^c \left[\sum_{m=0}^{\infty} \exp(-|y-v|\gamma_m^{(i)}) \cos(k_m z)\right] \operatorname{sgn}(y-v)\, Y(v,0)\,dv$$

$$= \int_b^c \Upsilon_c^{(i)}(|y-v|, z) \operatorname{sgn}(y-v)\,[Y(v,0) - Y(y,0)]\,dv$$

$$+ Y(y,0)\,[\Lambda_c^{(i)}(c-y, z) - \Lambda_c^{(i)}(y-b, z)], \tag{100}$$

$$\int_b^c \left[\sum_{m=0}^{\infty} \exp(-|y-v|\gamma_m^{(i)}) \sin(k_m z)\right] Y(v,0)\,dv$$

$$= \int_b^c \Upsilon_s^{(i)}(|y-v|, z)\,[Y(v,0) - Y(y,0)]\,dv + Y(y,0)\left[d - \Lambda_s^{(i)}(y-b, z)\right.$$

$$\left. - \Lambda_s^{(i)}(c-y, z) - 2i\kappa_i \sum_{m=0}^{\infty} \frac{\sin(k_m z)}{k_m \gamma_m^{(i)}(k_m + \gamma_m^{(i)})}\right], \tag{101}$$

where

$$\Lambda^{(i)}_{\{s\}^c}(\epsilon, z) = \sum_{m=0}^{\infty} \frac{\exp(-\epsilon\gamma_m^{(i)})}{\gamma_m^{(i)}} \begin{Bmatrix}\cos\\ \sin\end{Bmatrix}(k_m z),$$

$$\Upsilon^{(i)}_{\{s\}^c}(\epsilon, z) = \sum_{m=0}^{\infty} \exp(-\epsilon\gamma_m^{(i)}) \begin{Bmatrix}\cos\\ \sin\end{Bmatrix}(k_m z). \tag{102}$$

In obtaining the terms $d(d-z)\,Y(y,0)$ and $dY(y,0)$ in (99) and (101), respectively, we have used the well-known Fourier series expansions (see e.g. Dwight 1961, 416.10 and 416.01)

$$\frac{\pi}{8}(\pi - 2x) = \sum_{m=0}^{\infty} \frac{\cos[(2m+1)x]}{(2m+1)^2} \quad (0 \leqslant x \leqslant \pi), \qquad \frac{\pi}{4} = \sum_{m=0}^{\infty} \frac{\sin[(2m+1)x]}{2m+1} \quad (0 < x < \pi).$$

Explicit expressions for the series $\Lambda^{(i)}$ and $\Upsilon^{(i)}$ which reveal the nature of their singularities at $\epsilon = 0$ can be found by introducing the function

$$K_m^{(i)}(\epsilon) = 1 - \frac{i\kappa_i\epsilon}{k_m + \gamma_m^{(i)}} - \exp\left(-\frac{i\kappa_i\epsilon}{k_m + \gamma_m^{(i)}}\right) \tag{103}$$

and noting with the aid of (34) the following identities

$$\frac{\exp(-\epsilon\gamma_m^{(i)})}{\gamma_m^{(i)}} \equiv \left[\frac{1}{k_m} - \frac{i\kappa_i(1+k_m\epsilon)}{k_m\gamma_m^{(i)}(k_m+\gamma_m^{(i)})} - \frac{K_m^{(i)}(\epsilon)}{\gamma_m^{(i)}}\right] \exp(-k_m\epsilon)$$

$$\exp(-\epsilon\gamma_m^{(i)}) \equiv \left[1 - \frac{i\kappa_i\epsilon}{2k_m} - \frac{\kappa_i^2\epsilon}{2k_m(k_m+\gamma_m^{(i)})^2} - K_m^{(i)}(\epsilon)\right] \exp(-k_m\epsilon). \tag{104}$$

The coefficients of $\exp(-k_m\epsilon)$ given by the last two terms in the brackets on the right hand sides of these two identities are at least $O(1/k_m^2)$ and therefore yield series that converge fairly rapidly when substituted in (102). Only the first terms in the identities give slowly convergent series in the forms defined by

$$\bar{\Upsilon}(\epsilon, z) \equiv \bar{\Upsilon}_c(\epsilon, z) + i\bar{\Upsilon}_s(\epsilon, z) = \sum_{m=0}^{\infty} \exp[-k_m(\epsilon - iz)] \tag{105}$$

$$\bar{\Lambda}(\epsilon, z) \equiv \bar{\Lambda}_c(\epsilon, z) + i\bar{\Lambda}_s(\epsilon, z) = \sum_{m=0}^{\infty} \frac{\exp[-k_m(\epsilon - iz)]}{k_m} = \int_{\epsilon}^{\infty} \bar{\Upsilon}(\epsilon, z)\, d\epsilon. \tag{106}$$

Since $k_m = (2m+1)\pi/2d$, the final expression in (105) can be summed as a geometric series to give

$$\bar{\Upsilon}(\epsilon, z) = \frac{\exp[-\pi(\epsilon - iz)/2d]}{1 - \exp[-\pi(\epsilon - iz)/d]} \tag{107}$$

and the integration prescribed by (106) then gives

$$\bar{\Lambda}(\epsilon, z) = \frac{d}{\pi} \log\left(\frac{1 + \exp[-\pi(\epsilon - iz)/2d]}{1 - \exp[-\pi(\epsilon - iz)/2d]}\right). \tag{108}$$

Both these expressions become infinite as $\epsilon \to 0$ and $z \to 0$ but the singularities are sufficiently weak that when $z = 0+$ the integrands on the rhs of equations (99) and (100) both remain finite at the point $v = y$, with

$$\lim_{v \to y} \Lambda_c^{(i)}(|y - v|, 0+)\,[Y(v, 0) - Y(y, 0)] = 0,$$

$$\lim_{v \to y} \Upsilon_c^{(i)}(|y - v|, 0+)\,\mathrm{sgn}(y - v)\,[Y(v, 0) - Y(y, 0)] = -\frac{d}{\pi}\frac{\partial Y(y, 0)}{\partial y}. \tag{109}$$

Substitution of the identities (104) into (102) gives

$$\Lambda^{(i)}_{\{s\}^c}(\epsilon, z) = \begin{Bmatrix}\mathrm{Re}\\ \mathrm{Im}\end{Bmatrix} \bar{\Lambda}(\epsilon, z) - i\kappa_i \sum_{m=0}^{\infty} \frac{(1 + k_m\epsilon)\exp(-k_m\epsilon)}{\gamma_m^{(i)} k_m(k_m + \gamma_m^{(i)})} \begin{Bmatrix}\cos\\ \sin\end{Bmatrix}(k_m z)$$
$$- \sum_{m=0}^{\infty} \frac{K_m^{(i)}(\epsilon)}{\gamma_m^{(i)}} \exp(-k_m\epsilon) \begin{Bmatrix}\cos\\ \sin\end{Bmatrix}(k_m z) \tag{110}$$

$$\Upsilon^{(i)}_{\{s\}^c}(\epsilon, z) = \begin{Bmatrix}\mathrm{Re}\\ \mathrm{Im}\end{Bmatrix} \bar{\Upsilon}(\epsilon, z) - \frac{i\kappa_i\epsilon}{2} \begin{Bmatrix}\mathrm{Re}\\ \mathrm{Im}\end{Bmatrix} \bar{\Lambda}(\epsilon, z) - \frac{\kappa_i^2\epsilon}{2} \sum_{m=0}^{\infty} \frac{\exp(-k_m\epsilon)}{k_m(k_m + \gamma_m^{(i)})^2} \begin{Bmatrix}\cos\\ \sin\end{Bmatrix}(k_m z)$$
$$- \sum_{m=0}^{\infty} K_m^{(i)}(\epsilon) \exp(-k_m\epsilon) \begin{Bmatrix}\cos\\ \sin\end{Bmatrix}(k_m z)$$

which together with (103), (107) and (108) are in a form that can be readily evaluated even for small ϵ.

A similar problem is encountered in the computation of $\bar{G}_{ij}$ and $\bar{\Gamma}_{ij}$ when $\mathscr{S}_i$ and $\mathscr{S}_j$ are adjoining regions, for in this case both y and v can approach the same boundary value $\pm a$, albeit from opposite directions. This time the singular terms are those involving the exponential functions in the expressions for $\bar{G}_{ij}$ and $\bar{\Gamma}_{ij}$ ($|i-j|=1$) as quoted in (52) and (55). They can be integrated for all y and v as follows:

$$\int_b^c \left[\sum_{m=0}^{\infty} \frac{\exp\left[\pm(v-y)\gamma_m^{(i)}\right]}{\gamma_m^{(i)}} \cos(k_m z) \right] Y(v,0)\, dv$$

$$= \int_b^c \Lambda_c^{(i)}\left[\pm(y-v), z\right]\left[Y(v,0) - Y(\bar{a},0)\right] dv$$

$$\pm Y(\bar{a},0) \sum_{m=0}^{\infty} \frac{\cos(k_m z)}{(\gamma_m^{(i)})^2} \left\{\exp\left[\pm(c-y)\gamma_m^{(i)}\right] - \exp\left[\pm(b-y)\gamma_m^{(i)}\right]\right\} \tag{111}$$

and

$$\int_b^c \left[\sum_{m=0}^{\infty} \exp\left[\pm(v-y)\gamma_m^{(i)}\right] \begin{Bmatrix}\cos\\ \sin\end{Bmatrix}(k_m z) \right] Y(v,0)\, dv$$

$$= \int_b^c \Upsilon^{(i)}_{\{s\}^c}\left[\pm(y-v), z\right]\left[Y(v,0) - Y(\bar{a},0)\right] dv$$

$$\pm Y(\bar{a},0)\left\{\Lambda^{(i)}_{\{s\}^c}\left[\pm(y-c), z\right] - \Lambda^{(i)}_{\{s\}^c}\left[\pm(y-b), z\right]\right\}, \tag{112}$$

where $\bar{a}$ stands for either $+a$ or $-a$ whichever is the common boundary value of y and v.

We write the electric field in the form

$$U(y,z) = \tilde{U}(y,z) + U^*(y,z) + i\omega(d-z)\, Y(y,0), \tag{113}$$

where $\tilde{U}$ is that part of the field arising from the terms $A_m^{(l)}$, $C_m^{(l)}$, $L_m^{+(l)}$, $M_m^{(l)}$ and $N_m^{(l)}$ defined in (46)–(50) while the remaining part represents the contribution from the singular terms in the Green's function. The function $U_i^* \equiv U^*[(y,z) \in \mathscr{S}_i,\ i = 1, 2, 3]$ can be found for $i = 1$ by considering just the last terms in the expressions for $\bar{G}_{11}$ and $\bar{G}_{12}$ given in (55). Setting $b = -\infty$, $c = -a$ in (99) and $b = -a$, $c = a$ in (111) with the negative sign taken in the argument of the exponential function and $\bar{a} = -a$, we obtain

$$U_1^* = \frac{i\omega}{d}\left(\int_{-\infty}^{-a} \Lambda_c^{(1)}(|y-v|, z)\left[Y(v,0) - Y(y,0)\right] dv\right.$$

$$+ \int_{-a}^{a} \Lambda_c^{(1)}(v-y, z)\left[Y(v,0) - Y(-a,0)\right] dv$$

$$- \sum_{m=0}^{\infty} \frac{\cos(k_m z)}{(\gamma_m^{(1)})^2}\left[\frac{2ik_1}{k_m^2} Y(y,0) + Y(-a,0)\exp\left[(y+a)\gamma_m^{(1)}\right]\right.$$

$$\left.\left. + \left[Y(y,0) - Y(-a,0)\right]\exp\left[(y+a)\gamma_m^{(1)}\right]\right]\right). \tag{114}$$

Similarly for $i = 2$, we put $b = -a$, $c = a$ in (99), and both $b = -\infty$, $c = -a$, $\bar{a} = -a$, and $b = a$, $c = \infty$, $\bar{a} = a$ in (111) with respectively positive and negative signs in the argument of the exponential function. This gives

$$U_2^* = \frac{i\omega}{d}\left[\int_{-\infty}^{-a} \Lambda_c^{(2)}(y-v,z)\,[Y(v,0)-Y(-a,0)]\,dv\right.$$
$$+\int_{-a}^{a} \Lambda_c^{(2)}(|y-v|,z)\,[Y(v,0)-Y(y,0)]\,dv$$
$$+\int_{a}^{\infty} \Lambda_c^{(2)}(v-y,z)\,[Y(v,0)-Y(a,0)]\,dv$$
$$-\sum_{m=0}^{\infty}\frac{\cos(k_m z)}{(\gamma_m^{(2)})^2}\left[\frac{2i\kappa_2}{k_m^2}\,Y(y,0)+[Y(y,0)-Y(-a,0)]\exp[-(y+a)\gamma_m^{(2)}]\right.$$
$$\left.\left.+[Y(y,0)-Y(a,0)]\exp[(y-a)\gamma_m^{(2)}]\right]\right]. \tag{115}$$

Finally, with $i = 3$, $b = a$, $c = \infty$ in (99), and $b = -a$, $c = a$, $\bar{a} = a$, and positive argument of the exponential function in (111) we obtain

$$U_3^* = \frac{i\omega}{d}\left[\int_{-a}^{a} \Lambda_c^{(3)}(y-v,z)\,[Y(v,0)-Y(a,0)]\,dv\right.$$
$$+\int_{a}^{\infty} \Lambda_c^{(3)}(|y-v|,z)\,[Y(v,0)-Y(y,0)]\,dv$$
$$-\sum_{m=0}^{\infty}\frac{\cos(k_m z)}{(\gamma_m^{(3)})^2}\left[\frac{2i\kappa_3}{k_m^2}\,Y(y,0)+Y(a,0)\exp[-(a+y)\gamma_m^{(3)}]\right.$$
$$\left.\left.+[Y(y,0)-Y(a,0)]\exp[(a-y)\gamma_m^{(3)}]\right]\right]. \tag{116}$$

The calculation of the vertical magnetic field given by (19) is handled in like manner by defining $\tilde{Z}$ analogously to $\tilde{U}$ in (113) and writing

$$Z(y,z) = \tilde{Z}(y,z) + Z^*(y,z).$$

It has already been noted in Section 4 that the infinite series contributing to $\tilde{Z}$ are convergent everywhere, so that the evaluation of that part of the field is a straightforward computation. The singular terms are treated with the aid of (100) and (112) in exactly the same way as those in the expressions for $\bar{G}_{ij}$. Noting that $\Lambda_c^{(i)}(\infty,z) = 0$ we obtain $Z_i^* \equiv Z^*[(y,z)\in\mathscr{S}_i; i = 1,2,3]$ in the form:

$$Z_1^* = -\frac{1}{d}\left[\int_{-\infty}^{-a} \Upsilon_c^{(1)}(|y-v|,z)\,\mathrm{sgn}(y-v)\,[Y(v,0)-Y(y,0)]\,dv\right.$$
$$-\int_{-a}^{a} \Upsilon_c^{(1)}(v-y,z)\,[Y(v,0)-Y(-a,0)]\,dv$$
$$\left.+Y(-a,0)\,\Lambda_c^{(1)}(a-y,z)+[Y(y,0)-Y(-a,0)]\,\Lambda_c^{(1)}(-y-a,z)\right], \tag{117}$$

$$Z_2^* = -\frac{1}{d}\left[\int_{-\infty}^{-a} \Upsilon_c^{(2)}(y-v,z)\,[Y(v,0)-Y(-a,0)]\,dv\right.$$

$$+\int_{-a}^{a} \Upsilon_c^{(2)}(|y-v|,z)\,\mathrm{sgn}\,(y-v)\,[Y(v,0)-Y(y,0)]\,dv$$

$$-\int_{a}^{\infty} \Upsilon_c^{(2)}(v-y,z)\,[Y(v,0)-Y(a,0)]\,dv$$

$$\left.-[Y(y,0)-Y(-a,0)]\Lambda_c^{(2)}(y+a,z)+[Y(y,0)-Y(a,0)]\Lambda_c^{(2)}(a-y,z)\right], \quad (118)$$

$$Z_3^* = -\frac{1}{d}\left[\int_{-a}^{a} \Upsilon_c^{(3)}(y-v,z)\,[Y(v,0)-Y(a,0)]\,dv\right.$$

$$+\int_{a}^{\infty} \Upsilon_c^{(3)}(|y-v|,z)\,\mathrm{sgn}\,(y-v)\,[Y(v,0)-Y(y,0)]\,dv$$

$$\left.-Y(a,0)\,\Lambda_c^{(3)}(y+a,z)-[Y(y,0)-Y(a,0)]\,\Lambda_c^{(3)}(y-a,z)\right]. \quad (119)$$

Note that although $\Lambda_c^{(i)}(\epsilon,0)$ is logarithmically singular (see (110) and (108)) when $\epsilon = 0$ the coefficients of the final terms in (117)–(119) all vanish at the points of singularity and so cause these terms to drop out.

By analogy with (113) we express the horizontal magnetic field in the form

$$Y(y,z) = \tilde{Y}(y,z) + Y^*(y,z) + Y(y,0).$$

It is calculated from the integral (18) where G' is given by (53). This time the contributions to $Y^*(y,z) + Y(y,0)$ arise from the final terms in the Green's functions $k_m \bar{G}_{ij}$ and take the form

$$\frac{k_m}{\gamma_m^{(i)}}\exp\left[\pm(y-v)\gamma_m^{(i)}\right] \equiv \left[1-\frac{ik_i}{\gamma_m^{(i)}(k_m+\gamma_m^{(i)})}\right]\exp\left[\pm(y-v)\gamma_m^{(i)}\right]. \quad (120)$$

The second term on the rhs of this identity is $O(1/k_m^2)$ when $v = y$ and so presents no convergence problems when substituted in (53). However, we retain it as part of the contribution to Y^* so that $\tilde{Y}$ (like $\tilde{U}$ and $\tilde{Z}$) is associated solely with the terms $A_m^{(I)}$, $C_m^{(I)}$, $L_m^{+(I)}$, $M_m^{(I)}$ and $N_m^{(I)}$ appearing in the Green's functions. Following the usual procedure we calculate Y_1^* by considering the singular terms in $k_m\bar{G}_{11}$ and $k_m\bar{G}_{12}$. First we use the identity (120), and then set $b = -\infty$, $c = -a$ in (101) and $b = -a$, $c = a$ in (112) with $\bar{a} = -a$ and the negative sign taken in the argument of the exponential. Corresponding procedures are used to find Y_2^* and Y_3^*. We may write the resulting expressions for $i = 1, 2, 3$ as

$$Y_i^* = Y_i^{**} - \frac{ik_i}{d}\left(Y(y,0)\sum_{m=0}^{\infty}\left[\frac{2}{k_m}-\frac{\exp\left[(b_i-y)\gamma_m^{(i)}\right]}{k_m+\gamma_m^{(i)}}-\frac{\exp\left[(y-c_i)\gamma_m^{(i)}\right]}{k_m+\gamma_m^{(i)}}\right]\frac{\sin(k_m z)}{(\gamma_m^{(i)})^2}\right.$$

$$\left.+\int_{b_i}^{c_i}\left[\sum_{m=0}^{\infty}\frac{\exp\left(-|y-v|\gamma_m^{(i)}\right)\sin(k_m z)}{\gamma_m^{(i)}(k_m+\gamma_m^{(i)})}\right][Y(v,0)-Y(y,0)]\,dv\right). \quad (121)$$

where we have defined the limits of integration

$$b_1 = b_2 = -\infty, \quad b_3 = -a, \quad c_1 = a, \quad c_2 = c_3 = \infty$$

and where evaluation of a rather slowly converging series at $v = y$ has been avoided by subtracting $Y(y, 0)$ from $Y(v, 0)$ in the integrand and adding the equivalent term, which can be integrated exactly, to the rapidly convergent series outside the integral. The expressions for Y_i^{**} $(i = 1, 2, 3)$ are given by

$$\begin{aligned} Y_1^{**} = \frac{1}{d} \Bigg[& \int_{-\infty}^{-a} \Upsilon_s^{(1)}(|y - v|, z)\, [Y(v, 0) - Y(y, 0)]\, dv \\ & + \int_{-a}^{a} \Upsilon_s^{(1)}(v - y, z)\, [Y(v, 0) - Y(-a, 0)]\, dv \\ & + [Y(-a, 0) - Y(y, 0)]\, \Lambda_s^{(1)}(-a - y, z) - Y(-a, 0)\, \Lambda_s^{(1)}(a - y, 0) \Bigg], \end{aligned} \tag{122}$$

$$\begin{aligned} Y_2^{**} = \frac{1}{d} \Bigg[& \int_{-\infty}^{-a} \Upsilon_s^{(2)}(y - v, z)\, [Y(v, 0) - Y(-a, 0)]\, dv \\ & + \int_{-a}^{a} \Upsilon_s^{(2)}(|y - v|, z)\, [Y(v, 0) - Y(y, 0)]\, dv \\ & + \int_{a}^{\infty} \Upsilon_s^{(2)}(v - y, z)\, [Y(v, 0) - Y(a, 0)]\, dv \\ & + [Y(-a, 0) - Y(y, 0)]\, \Lambda_s^{(2)}(y + a, z) \\ & + [Y(a, 0) - Y(y, 0)]\, \Lambda_s^{(2)}(a - y, z) \Bigg], \end{aligned} \tag{123}$$

$$\begin{aligned} Y_3^{**} = \frac{1}{d} \Bigg[& \int_{-a}^{a} \Upsilon_s^{(3)}(y - v, z)\, [Y(v, 0) - Y(a, 0)]\, dv \\ & + \int_{a}^{\infty} \Upsilon_s^{(3)}(|y - v|, z)\, [Y(v, 0) - Y(y, 0)]\, dv \\ & + [Y(a, 0) - Y(y, 0)]\, \Lambda_s^{(3)}(y - a, z) - Y(a, 0)\, \Lambda_s^{(3)}(y + a, z) \Bigg]. \end{aligned} \tag{124}$$

7 Improved derivative formulae for finite difference calculations

In paper I we remarked that for easy comparison of the results given by the finite difference program of Brewitt-Taylor & Weaver (1976) with those provided by an analytic solution it is desirable to obtain new central difference formulae giving the derived field components at the nodes of the numerical grid rather than at the centre of the cells where they were calculated in the original version of the finite difference program. Because the horizontal electric component of the B-polarization field discussed in paper I was discontinuous at a vertical interface between regions of different conductivity, the final formulae as well as the

algebra involved in their derivation were surprisingly complicated. Fortunately matters are much simpler in the case of E-polarization where all the field components are continuous across conductivity boundaries. The new formulae for the magnetic field components which were used in the finite difference calculations to be described in Section 8 are quoted here for reference.

The notation is the same as in paper I and in the paper by Brewitt-Taylor & Weaver. Thus we write $U_{m,n}$ for the electric field at the node (y_m, z_n) of the numerical grid, and we define $h_m = y_{m+1} - y_m$ and $k_n = z_{n+1} - z_n$. The four conductivity values in the neighbouring cells are $\sigma_{m\pm1/2,n\pm1/2}$ as shown in Fig. 2 of paper I, and the weighted average values of the parameter κ in equation (3) at the points $(y_m, z_n - k_{n-1}/2)$, $(y_m, z_n + k_n/2)$, $(y_m - h_{m-1}/2, z_n)$ and $(y_m + h_m/2, z_n)$ are written $\kappa_{m,n-1/2}$, $\kappa_{m,n+1/2}$, $\kappa_{m-1/2,n}$ and $\kappa_{m+1/2,n}$ respectively and defined by

$$\kappa_{m,n\pm1/2} = (h_{m-1}\kappa_{m-1/2,n\pm1/2} + h_m\kappa_{m+1/2,n\pm1/2})/(h_m + h_{m-1})$$

$$\kappa_{m\pm1/2,n} = (k_{n-1}\kappa_{m\pm1/2,n-1/2} + k_n\kappa_{m\pm1/2,n+1/2})/(k_n + k_{n-1}).$$

Expanding the electric field U as a Taylor series (up to and including 2nd order terms) in the positive y-direction from the node (y_m, z_n) while regarding $y = y_m$ as a sharp boundary between regions of (possibly) different conductivities, we obtain, with the help of the second Maxwell equation (2) and the differential equation (3),

$$U_{m+1,n} = (1 + ih_m^2\kappa_{m+1/2,n})\,U_{m,n} + i\omega h_m Z_{m,n} - h_m^2(\partial^2 U/\partial z^2)_{m,n}. \tag{125}$$

All the field quantities in (125) are continuous across the boundary $y = y_m$ even though the second derivative $\partial^2 U/\partial y^2$ appearing in the original Taylor series expansion is discontinuous across this boundary when the two regions it divides are of different conductivity (as can be seen from the second and third Maxwell equations (2)). A similar equation (125) can be found by expanding U in the negative y-direction from the same node. Elimination of $(\partial^2 U/\partial z^2)_{m,n}$ from the two equations so obtained then yields, after some algebraic rearrangement, the required central difference formula

$$i\omega Z_{m,n} = \frac{h_m h_{m-1}}{h_m + h_{m-1}}\left[\left[\frac{U_{m+1,n}}{h_m^2} - \frac{U_{m-1,n}}{h_{m-1}^2}\right] - \left[\frac{1}{h_m^2} - \frac{1}{h_{m-1}^2} + \frac{i}{2}(\kappa_{m+1/2,n} - \kappa_{m-1/2,n})\right]U_{m,n}\right] \tag{126}$$

for the vertical magnetic field. Starting with Taylor expansions in the positive and negative z-directions we can develope an analogous formula for the horizontal magnetic field in the form

$$i\omega Y_{m,n} = -\frac{k_n k_{n-1}}{k_n + k_{n-1}}\left[\left[\frac{U_{m,n+1}}{k_n^2} - \frac{U_{m,n-1}}{k_{n-1}^2}\right] - \left[\frac{1}{k_n^2} - \frac{1}{k_{n-1}^2} + \frac{i}{2}(\kappa_{m,n+1/2} - \kappa_{m,n-1/2})\right]U_{m,n}\right]. \tag{127}$$

In regions of uniform conductivity, the rhs of (126) and (127) reduce to the standard central difference formulae for first derivatives (cf. formula (128) in the following Section 8) as required by the Maxwell equations (2). At the surface of the earth $z = 0$ where $n = q$ (say) and $\kappa_{m,q-1/2} = 0$, the resulting simplified form of (127) agrees with a special formula derived by Brewitt-Taylor & Weaver (their equation (6.10)) for evaluating Y at the surface nodes.

8 Numerical calculations

For a comparison of results given by the finite difference program of Brewitt-Taylor & Weaver (1976) and finite element program of Kisak & Silvester (1975) with the quasi-analytic solution derived in this paper, the model parameters used were the same as in Paper I i.e. $a = 10$ km, $d = 50$ km, $\sigma_1 = 0.1$ S m^{-1}, $\sigma_2 = 1.0$ S m^{-1}, $\sigma_3 = 0.5$ S m^{-1} and period $T \equiv 2\pi/\omega = 300$ s, as shown in Fig. 1.

For the analytic solution the functions Ξ and h were computed according to formulae (69)–(71) and (82) with the special cases (89), (90) and (93)–(96) taken into account. The use of the identity (75) for summing the functions g was found to be extremely important. The integral in (32) was evaluated between $v = \mp v_1$ by Simpson's rule with the intervals $(-v_1, -v_0), (-v_0, -a), (-a, a), (a, v_0)$ and (v_0, v_1) respectively divided into N_2, N_1, N_0, N_1 and N_2 subintervals each of width Δ_0 between $-v_0$ and $+v_0$, and of width Δ between $-v_1$ and $-v_0$ and between v_0 and v_1. The remaining parts of the integral covering the intervals $(-\infty, -v_1)$ and (v_1, ∞) were evaluated by 8-point Gauss–Laguerre formulae. For the parameters listed above it was found that the values $v_1 = 53$ km, $v_0 = 15$ km, and $N_2 = 38$, $N_1 = 10$, $N_0 = 40$ (so that $\Delta_0 = 0.5$ km and $\Delta = 1.0$ km) gave satisfactory results. Numerical experiments with subdivisions of different sizes gave no change in the accuracy of the values of $Y(y, 0)$ up to the number of significant figures presented in Table 1. Convergence to a limit was deemed to have occurred when the maximum change in the field value at any point was less than 10^{-8}; this was achieved after 1409 iterations through the successive approximation scheme. However the maximum change was already less than 10^{-3} after only 354 iterations.

Exactly the same subdivisions and methods of numerical integration were used to evaluate the field components U and Z for $z \geqslant 0$ and Y for $z > 0$, as given by the formulae (114)–(119) and (121)–(124). The only point requiring some explanation occurs when the variable of integration v assumes the value of y in the integrals defining Z, for then according to the second of equations (109), the integrand reduces to $(1/\pi)\partial Y(y, 0)/\partial y$ and a suitable procedure for evaluating this derivative must be found. At the two points at the extremities of the Gauss–Laguerre integration (several hundreds of kilometres from the origin) it is assumed that $\partial Y(y, 0)/\partial y = 0$. At all other points except $y = \pm a$ it is sufficient to use the central difference representation of the first derivative.

$$[\Delta_1^2 Y(y + \Delta_2, 0) + (\Delta_2^2 - \Delta_1^2) Y(y, 0) - \Delta_2^2 Y(y - \Delta_1, 0)]/[\Delta_1 \Delta_2 (\Delta_1 + \Delta_2)], \tag{128}$$

(Δ_1 and Δ_2 are respectively the subdivision spacings to the left and right of the node y) since this formula is based on a parabolic fit through the field values at the three points centred on y, which is the same approximation that leads to the Simpson's rule formula used in the integration. The discontinuity in $\partial^2 Y/\partial y^2$ at a surface node lying on the boundary between two segments of different conductivities means that Y is not a very smooth function of y there. Thus it is not appropriate to fit a parabola at such a node; rather we expand Y in Taylor series to the right and left of the node, substitute for $\partial^2 Y/\partial y^2$ from the different diffusion equations (of the same form as (3)) satisfied by Y on either side of the boundary, and eliminate the continuous function $\partial^2 Y/\partial z^2$ from the resulting equations, to obtain

$$[\partial Y(y, 0)/\partial y]_{y = \pm a} = [Y(\pm a + \Delta_0, 0) - Y(\pm a - \Delta_0, 0)]/2\Delta_0 \pm (i\Delta_0/4)(\kappa_2 - \kappa_\pm) Y(\pm a, 0)$$

where we have written $\kappa_+ \equiv \kappa_3$ and $\kappa_- \equiv \kappa_1$. It is clear that the second term represents a correction to the normal central difference formula.

Numerical values of the field components obtained from the analytic solution are dis-

Table 1. Values of the real and imaginary parts of the field components calculated from the analytic solution for selected points on the surface $z = 0$ and the interior plane $z = 15$ km of the model shown in Fig. 1. The units of U/B_0 are $V m^{-1} T^{-1}$; for comparison with results submitted to COMMEMI the (complex) values of U/B_0 should be divided by $310 + 295i$.

	U/B_0		$Y/B_0 \times 10^2$		$Z/B_0 \times 10^3$	
y(km)	Re	Im	Re	Im	Re	Im
z = 0 km						
-52	249	294	90.4	4.75	- 28.8	69.7
-25	194	247	86.3	- 1.60	-175	117
-15	171	196	92.9	- 7.29	-335	87.5
-10	166	154	114	- 3.09	-484	- 8.0
- 7	162	129	129	- 0.78	-321	90.6
0	147	102	131	- 9.21	- 79.3	92.1
7	138	102	124	- 9.47	73.4	40.8
10	135	108	116	- 9.89	146	54.0
15	133	120	106	- 9.28	77.9	- 0.1
30	136	130	103	- 3.96	7.5	- 8.0
50	137	130	103	- 2.71	- 1.8	2.1
z = 15 km						
-52	206	86.7	43.3	-25.4	- 4.8	67.5
-25	143	59.3	35.4	-23.9	-128	166
-15	102	19.5	24.4	-25.8	-264	230
-10	75.2	-13.0	12.6	-28.3	-359	285
- 7	57.9	-30.1	4.98	-29.2	-193	259
0	30.1	-41.5	- 3.32	-27.8	- 0.8	111
7	24.8	-36.9	- 2.54	-27.0	55.9	- 34.4
10	28.6	-32.7	0.37	-27.2	79.0	- 85.3
15	36.4	-26.5	5.10	-27.5	41.1	- 63.0
30	48.0	-22.8	9.41	-28.6	- 3.3	- 16.6
50	50.2	-24.4	9.95	-29.0	- 1.7	0.5

played in Table 1 to 3 significant figures. In numerical experiments only the results for Z at $y = \pm 10$ km on $z = 0$ appeared to be sensitive to the size of subdivision used. These particular values may have small errors of less than 1 per cent of B_0 but all the other results are accurate to the number of figures given. They are tabulated for the same selected points (both on the surface $z = 0$ and on the interior plane $z = 15$ km) that were chosen for the B-polarization calculations presented in paper I. They can be compared with the corresponding values in Table 2 given by the finite difference program of Brewitt-Taylor & Weaver (1976) (incorporating the improved derivative formulae developed in Section 7) and those in Table 3 given by the finite element program of Kisak & Silvester (1975).

For the finite difference calculations a 36 x 26 grid was designed with nodes at $y = -130$, -110, -90, -80, -70, -61, -52, -43, -34, -25, -19, -15, -12, -10, -8.5, -7, -5, -2.5, 0, 2.5, 5, 7, 8.5, 10, 12, 15, 18, 22, 26, 30, 34, 38, 43, 50, 60, 70 km and $z = -90$, -70, -50, -35, -20, -12, -8, -5, -3, -1.5, 0, 1.5, 3, 5, 7.5, 10, 12.5, 15, 17.5, 20, 24, 28, 32, 40, 45, 50 km. Apart from 10 additional rows extending the grid into the region $z < 0$, and one extra node at the right hand boundary of the model, this is the same grid that was used in paper I. The asymptotic boundary conditions of Weaver & Brewitt-Taylor

Table 2. As in Table 1 except that the field components are calculated by the finite difference program of Brewitt-Taylor & Weaver (1976).

		U/B_o		$Y/B_o \times 10^2$		$Z/B_o \times 10^3$	
	y(km)	Re	Im	Re	Im	Re	Im
z = 0 km							
	-52	249	293	90.4	4.57	- 31.0	68.9
	-25	195	247	86.2	- 1.75	-180	115
	-15	172	195	92.6	- 7.45	-340	83.0
	-10	166	153	113	- 3.36	-483	- 9.7
	- 7	163	128	130	- 0.39	-325	86.6
	0	148	100	132	- 9.03	- 80.6	91.4
	7	138	100	124	- 9.25	74.7	42.6
	10	136	107	116	-10.0	145	55.8
	15	134	118	106	- 9.29	79.5	1.7
	30	137	129	103	- 3.99	8.5	- 7.7
	50	137	129	103	- 2.61	- 0.4	3.6
z = 15 km							
	-52	205	85.5	43.4	-25.4	-6.7	67.8
	-25	143	58.9	35.6	-23.9	-132	167
	-15	102	19.2	24.7	-25.8	-266	232
	-10	75.1	-13.4	13.0	-28.4	-360	287
	- 7	57.6	-30.4	5.34	-29.2	-194	260
	0	29.6	-41.3	-2.92	-27.8	- 1.9	111
	7	24.5	-36.7	-2.19	-27.0	55.3	-34.1
	10	28.3	-32.6	0.69	-27.1	78.3	-85.0
	15	36.0	-26.5	5.35	-27.5	41.1	-62.9
	30	47.5	-23.0	9.57	-28.5	- 2.9	-16.9
	50	49.7	-24.4	10.2	-28.9	- 1.6	- 0.3

(1978) were included in the program. It was for this reason the extra node at $y = 70$ km was inserted, for the program continues to store the 1-D analytic solutions (valid at $y = \pm \infty$) in the columns at the edges of the model and they do not properly match the computed field values at the neighbouring interior nodes when asymptotic boundary conditions are used. The inclusion of an extra node at $y = 70$ km effectively removes the 1-D solutions from the calculation of the horizontal derivative of U (i.e. the field Z) at $y = 50$ km.

The triangulation scheme used in the implementation of the finite element program is shown in Fig. 3. In $z > 0$ it is the same as in paper I. Only one strip of triangular elements is shown in $z < 0$ since the program automatically adds a specified number of identical strips above it to cover the region adequately. A total of 3 such strips were included in our calculations which put the upper boundary of the model at a height of 90 km (or about 3 skin-depths of the left-hand segment).

Tables 1 and 2 reveal the remarkable accuracy of the finite difference calculations. The errors in the separate real and imaginary parts of the magnetic field are less than 1 per cent relative to B_0 and the corresponding errors in the electric field are always less than (and generally much less than) 1.1 per cent relative to a typical magnitude of the electric field for the region in question (i.e. the surface fields at $y = -\infty$, 0 and $+\infty$ for regions 1, 2 and

Table 3. As in Table 1 except that the field components are calculated by the finite element program of Kisak & Silvester (1976). At points where numerical derivatives of the electric field can be obtained from the field values in two different triangular elements sharing a common vertex (see Fig. 3) the two values of the resulting magnetic field were not always found to be equal. In such cases both values are given. The magnetic field components at points inside the conducting slab are not provided by the finite element program.

		U/B_o		$Y/B_o \times 10^2$		$Z/B_o \times 10^3$	
	y(km)	Re	Im	Re	Im	Re	Im
z = 0 km							
	-52	245	287	89.6	4.89	- 18.2	58.1
	-25	193	241	85.5 86.5	-1.61 -1.93	-135 -138	115 116
	-15	170	190	92.6	-7.90	-284	101
	-10	165	151	100 113	-12.3 -5.27	-381	67.8 66.1
	- 7	161	126	131 130	-1.80 -1.09	-281 -264	101 108
	0	146	98.6	130 131	-10.9 -10.0	-63.0 -57.3	86.9 83.0
	7	138	98.8	126 125	- 9.84 -10.2	66.6 72.1	25.7 26.1
	10	135	105	118 117	- 9.47 -10.8	116 115	19.7 19.2
	15	134	116	107	-10.2 -10.3	73.0 64.9	-10.8 -11.7
	30	138	127	104	- 5.25	5.6	-10.5
	50	140	127	105	- 4.54	- 1.1	- 0.7
z = 15 km							
	-52	206	86.4				
	-25	144	58.8				
	-15	103	18.9				
	-10	75.7	-13.8				
	- 7	58.2	-30.9				
	0	30.0	-42.5				
	7	24.8	-37.8				
	10	28.7	-33.6				
	15	36.7	-27.6				
	30	48.7	-24.3				
	50	51.1	-26.3				

3 respectively). In the standard format recommended for the COMMEMI project (Zhdanov & Varentsov 1985) electric fields are normalized by E_0, the surface electric field at $y = -\infty$. A 1-D solution for the left hand segment of the control model gives $E_0/B_0 = 310.0 + 295.0i$, so that the tabulated (complex) values of U/B_0 should be divided by this complex number for comparison with COMMEMI data.

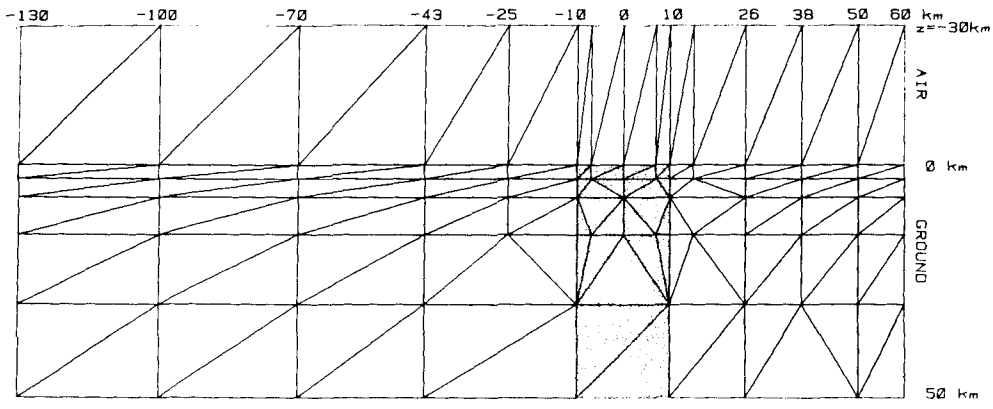

Figure 3. The triangulation scheme used in the application of the finite element program of Kisak & Silvester (1975). Only one of three identical strips covering the region above the earth is shown.

The results obtained from the finite element calculation presented in Table 3 are less satisfactory. Errors in the electric field are typically larger, ranging up to 1.7 per cent near the centre of the model and then actually getting worse as the right extremity of the grid is approached, which is exactly the opposite of what one would expect. For example at $y = 50$ km, $z = 0$ the relative error in both the real and imaginary parts of U/B_0 has reached 2.3 per cent, and a similar trend is also apparent along $z = 15$ km. Magnetic field values are tabulated only for points on the surface since, without modification, the program supplied by Kisak & Silvester does not permit the calculation of derived fields inside the conductor. Some of the selected points on the surface are at a common vertex of two different triangles, each of which can be used to calculate derivatives of the field at that point. Although the two values obtained should agree, in many cases they did not. At such points both values of the magnetic field are recorded in Table 3. The errors are again considerably larger than those generated by the finite difference program, especially at the boundary $y = -10$ km between the regions of high conductivity contrast where the error in the vertical magnetic field is almost 10 per cent.

A visual comparison of the results is provided by Figs 4 and 5 in which the variation of the real and imaginary parts of the field components across the planes $z = 0$ km and $z = 15$ km are plotted between $y = \pm 50$ km. For easy reference, the analytic curves are repeated as dotted lines superimposed on the graphs depicting the numerical results. It is at once apparent that the finite difference and analytic curves are barely distinguishable from each other; even the intricate cusp-like behaviour of the vertical magnetic field at $y = \pm 10$ km is fully and accurately reproduced by the finite difference calculations. The shortcomings of the finite element program are also made apparent in Figs 4 and 5. Both the relatively poor representation of the variation of the magnetic field components in the neighbourhood of $y = \pm 10$ km and the odd trend of the electric field as y increases, are clearly visible. We have attributed this latter behaviour to the (false) assumption made by Kisak & Silvester that U is constant (and equal to its value at $y = -\infty$) across the top of the grid. At height h it should really change smoothly between its different 1-D values of $i\omega B_0[(ik_j)^{-1/2} \tanh(d\sqrt{ik_j}) - h]$, $j = 1$ and 3, at $y = -\infty$ and $y = \infty$ respectively.

This conjecture was tested by making further calculations on the same model but with $\sigma_3 = 10^{-3}$ S m^{-1} (so that there was a much higher conductivity contrast between the left and right segments), and on a wider grid extending between $y = \mp 700$ km. This time it was found

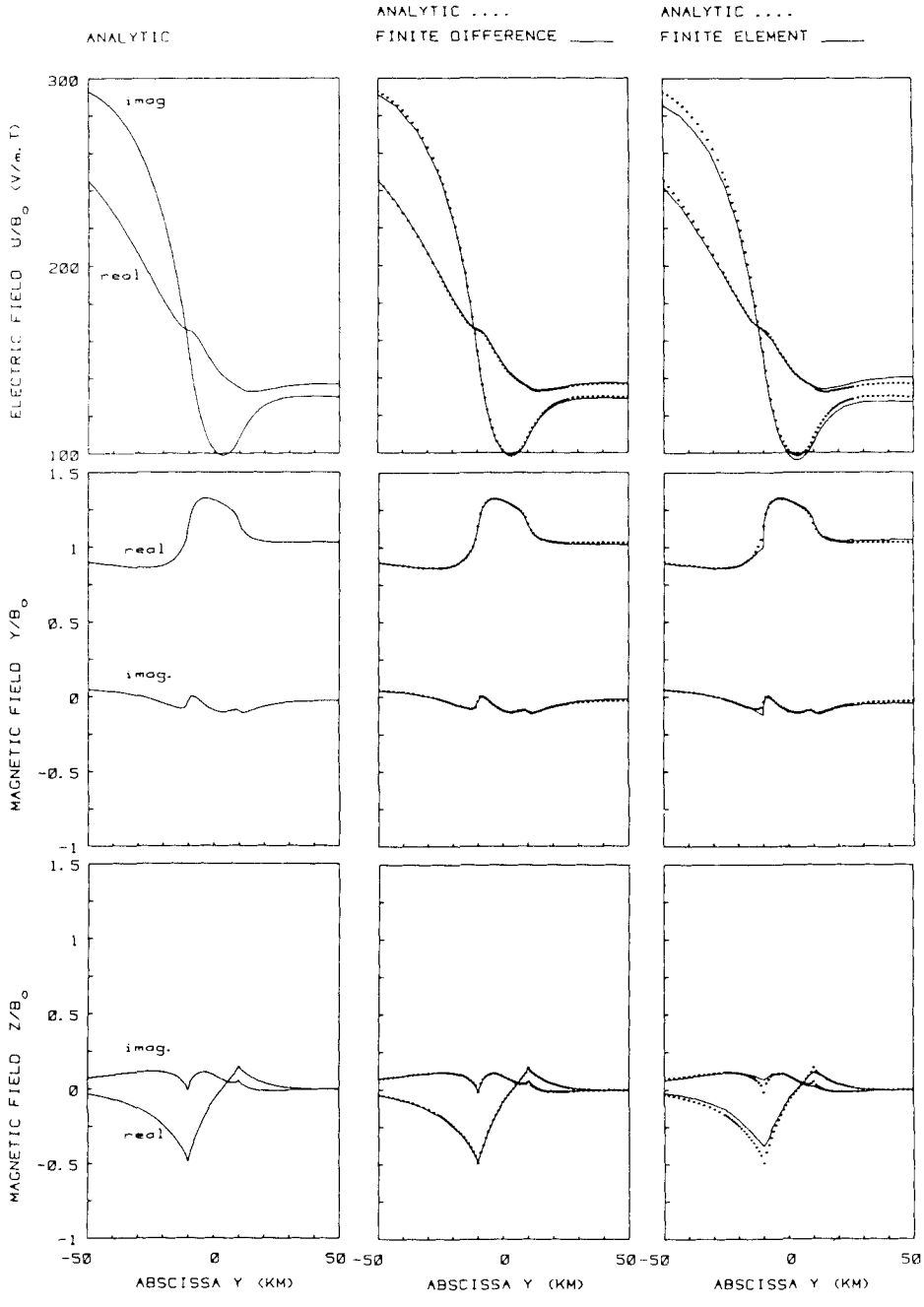

Figure 4. Comparison of the variations of the real and imaginary parts of the horizontal electric (U), horizontal magnetic (Y), and vertical magnetic (Z) fields along the surface $z = 0$ for the parameters shown in Fig. 1. The curves in the left hand column are those given by the analytic solution. They are reproduced as dotted lines in the other diagrams for easy comparison with the corresponding curves obtained from the finite difference program of Brewitt-Taylor & Weaver (1976) and the finite element program of Kisak & Silvester (1975) shown in the centre and right hand columns respectively.

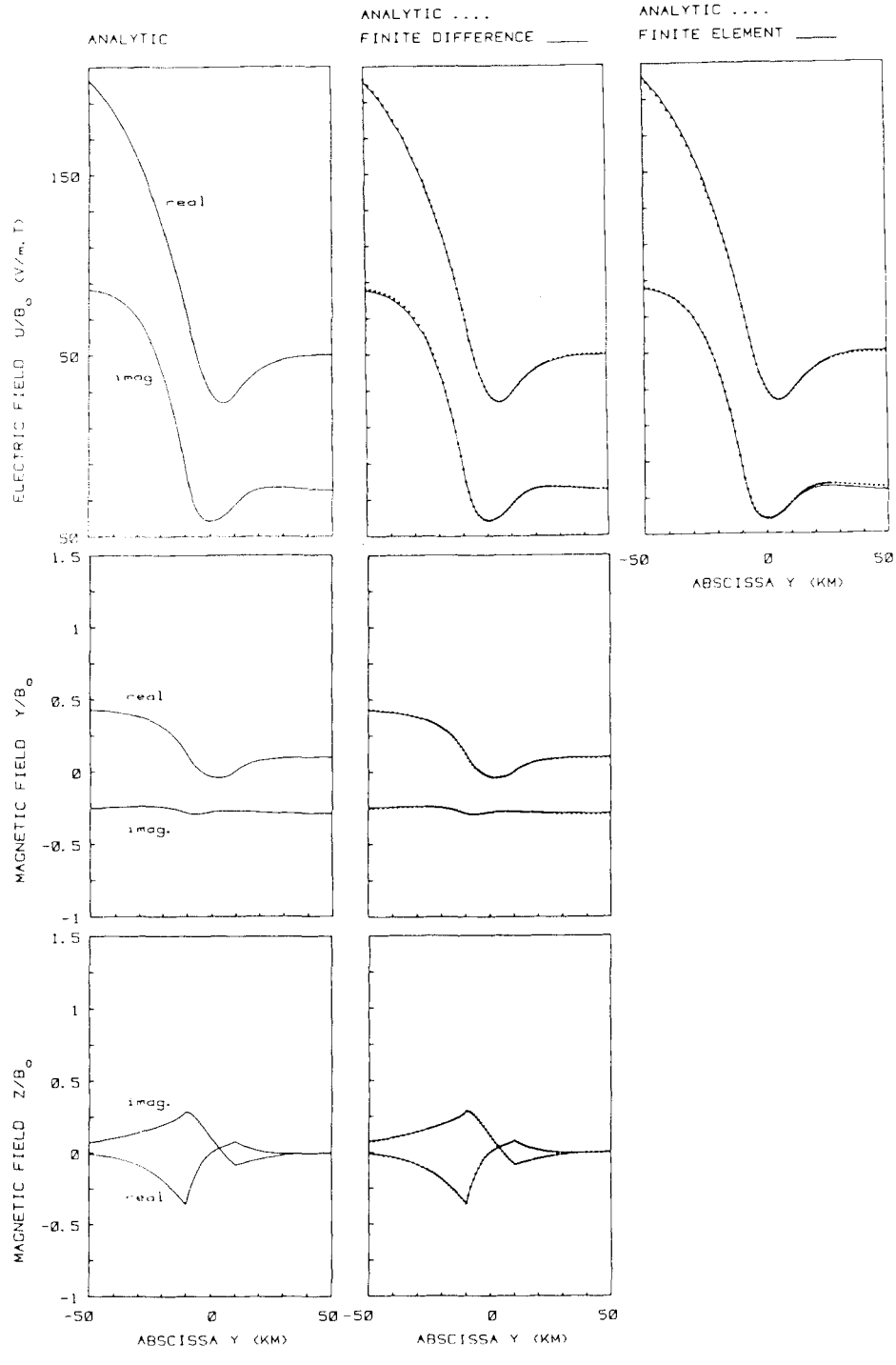

Figure 5. The same as in Fig. 4 except that the variations are along the interior horizontal plane at depth $z = 15$ km. Only the electric field is given at interior points by the finite element program.

that the discrepancies in the finite element (compared with the finite difference) values of U for large positive values of y were very much greater – up to 20 per cent – which is to be expected since the more widely differing values of κ_1 and κ_3 will affect the 1-D solutions in a corresponding manner. Similar errors were found in the Y-field but they tended to cancel out when the ratio U/Y was taken, so that the finite element program continued to give reasonably accurate values of apparent resistivity and phase. Clearly apparent resistivity is not a reliable indicator of how well a particular modelling program performs; it is important to calculate actual field values when comparing the accuracy of different numerical procedures.

Apart from the case when $\kappa_1 = \kappa_3$, Kisak & Silvester's assumption of constant U across the top of the grid is also approximately valid if h is so large that it dominates the term $(i\kappa_j)^{-1/2} \tanh (d\sqrt{i\kappa_j})$ in the 1-D solution. Thus the calculations were repeated once more with the same high conductivity contrast but now with each strip of triangular elements above the earth 300 km (rather than 30 km) thick. With three such strips included above the earth, the top of the finite element grid was now at a height of about 3 skin depths of the right-hand (low conductivity) segment rather than the left-hand (high conductivity) one. This modification did indeed correct the values of U at the edge of the model but only at the expense of new numerical inaccuracies arising near $y = 0$ (where the density of grid points is greatest) as a result of the triangular elements there becoming extremely thin and elongated. Further details on these calculations have been given by Weaver, LeQuang & Fischer (1984). We conclude that the finite element program of Kisak & Silvester is not able to cope well with models whose 1-D conductivity distributions at $y = \pm\infty$ are different.

It is hoped that the tabulated results in both this paper and paper I will serve as a useful check on the accuracy of the various modelling programs that have been developed in different institutions around the world. The analytic solutions can, of course, be calculated for different parameters a, d, σ_1, σ_2, σ_3, and ω. In particular d could be made large (several skin depths of the least conducting segment) to check programs that cannot easily accommodate perfect conductors or represent them by using a very large finite value for the conductivity.

Acknowledgments

This work is supported by grants from the Natural Sciences and Engineering Research Council of Canada, the Swiss National Science Foundation and the Geophysical Commission of the Academy of National Sciences (Switzerland). It was begun when one of us (J. T. Weaver) was a visitor to the Observatoire Cantonal de Neuchâtel on leave from the University of Victoria. Financial support from the Swiss National Science Foundation and the Canton de Neuchâtel which made this visit possible is gratefully acknowledged.

References

Brewitt-Taylor, C. R. & Weaver, J. T., 1976. On the finite difference solution of two-dimensional induction problems, *Geophys. J. R. astr. Soc.*, **47**, 375–396.

Dwight, H. B., 1961. *Tables of Integrals and Other Mathematical Data* (4th edition), Macmillan, New York.

Gautschi, W. & Cahill, W. F., 1964. Exponential integral and related functions, in *Handbook of Mathematical Functions*, eds Abramowitz, M. & Stegun, I. A., Nat. Bur. Stand., Washington, D.C.

Kisak, E. & Silvester, P., 1975. A finite element program package for magnetotelluric modelling, *Comp. Phys. Comm.*, **10**, 421–433.

Klügel, M., 1976. Berechnung der Elektromagnetischen Induktion in zwei Halbplatten zur Anwendung in der Magnetotellurik und erdmagnetischen Tiefensondierung, *Diplomarbeit*, Techn. Univ. Braunschweig, Inst. Geophys. Meteorol.

Klügel, M., 1977. Induction in plates with two-dimensional conductivity distribution, *Acta Geodaet. Geophys. et Montanist. Acad. Sci. Hung.*, **12**, 267–273.

Mann, J. E., 1970. A perturbation technique for solving boundary value problems arising in the electrodynamics of conducting bodies, *Appl. Sci. Res.*, **22**, 113–126.

Rodemann, H., 1978. Elektromagnetische Induktion in einer leitfähigen Platte mid eingelagertem vertikalem, endlichem Zylinder, *PhD thesis*, Techn. Univ. Braunschweig, Inst. Geophys. Meteorol. (Gamma **30**).

Schmucker, U., 1971. Interpretation of induction anomalies above non-uniform surface layers, *Geophys.* **36**, 156–165.

Sneddon, I. N., 1951. *Fourier Transforms*, McGraw-Hill, New York.

Treumann, R., 1970. Electromagnetic induction problem in plates with two-dimensional conductivity distribution: II. Approximate method and solutions, *Geomagn. Aeronom.*, **10**, 464–472.

Vladimirov, V. S., 1984. *Equations of mathematical analysis*, Mir Publishers, Moscow.

Weaver, J. T., 1963. The electromagnetic field within a discontinuous conductor with reference to geomagnetic micropulsations near a coastline, *Can. J. Phys.*, **41**, 484–495.

Weaver, J. T. & Brewitt-Taylor, C. R., 1978. Improved boundary conditions for the numerical solution of E-polarization problems in geomagnetic induction, *Geophys. J. R. astr. Soc.*, **54**, 309–317.

Weaver, J. T., LeQuang, B. V. & Fischer, G., 1984. Remarks on the comparison of analytical and numerical model calculations, in *Protokoll über das 10. Kolloquium 'Elektromagnetische Tiefenforschung'* (Grafrath/Oberbayern), pp. 219–235, eds Haak, V. (Berlin) & Homilius, J. (Hannover).

Weaver, J. T., LeQuang, B. V. & Fischer, G., 1985. A comparison of analytic and numerical results for a two-dimensional control model in electromagnetic induction – I. B-polarization calculations, *Geophys. J. R. astr. Soc.*, **82**, 263–277.

Weaver, J. T. & Thomson, D. W., 1972. Induction in a non-uniform conducting half-space by an external line current, *Geophys. J. R. astr. Soc.*, **28**, 163–185.

Weidelt, P., 1966. Modellrechnungen zur Deutung der norddeutschen Leitfähigheitsanomalie als oberflächennahe Leitfähigkeitsänderung, *Diplomarbeit*, Univ. Göttingen.

Zhdanov, M. S. & Varentsov, Iv.M., 1985. *Revised program of COMMEMI project*, document obtainable from Institute of Terrestrial Magnetism, Ionosphere and Radio Wave Propagation (IZMIRAN), U.S.S.R. Academy of Sciences, 142092 Troitsk, U.S.S.R.